A strategy to study pathway cross-talks of cells under repetitive exposure to stimuli

Xiaoshan Jiang

Thesis submitted to the faculty of the
Virginia Polytechnic Institute and State University
in partial fulfillment of the requirements for the degree of

Master of Science
In
Biological Sciences

Jianhua Xing, Chair
Iuliana M. Lazar
Jianyong Li

April 26, 2012
Blacksburg, Virginia

Keywords: High throughput, systems biology, regulatory network, mathematical model

A strategy to study pathway cross-talks of cells under repetitive exposure to stimuli

Xiaoshan Jiang

ABSTRACT

In each individual cell, there are many signaling pathways that may interact or cross talk with each other. Especially, some can sense the same signal and go through different pathways but eventually converge at some points. Therefore repetitive signal stimulations may result in intricate cell responses, among which the priming effect has been extensively studied in monocytes and macrophages as it plays an unambiguously crucial role in immunological protection against pathogen infection. Priming basically describes the phenomena that host cells can launch a dramatically enhanced response to the second higher dose of stimulus if cells have been previously treated with a lower dose of identical stimulus. It was reported to be associated with many human immune diseases (such as rheumatoid arthritis and hepatitis) that are attracting more and more researches on the priming effect. It is undoubtable that many genes are involved in this complicated biological process. Microarray is one of the standard techniques that are applied to do the transcriptome profiling of cells under repetitive stimuli and reveal gene regulatory networks. Therefore a well-established pipeline to analyze microarray data is of special help to investigate the underlying mechanism of priming effect. In this research, we aimed to design a strategy that can be used to interpret microarray data and to propose gene candidates that potentially participate in priming effect. To confirm our analysis results, we used a detailed mathematical model to further demonstrate the mechanism of a specific case of priming effect in a computational perspective.

DEDICATION

This thesis is dedicated to my parents, all the teachers and friends who have been always standing by to accompany me to grow up, to encourage me to overcome difficulties in life and to support me to be who I am now.

ACKNOWLEDGEMENTS

First of all, I would like to thank my advisor, Dr. Jianhua Xing for his constant help all through my application, transfer, study, research and graduation. Not only is his instruction an intellectual outreach for my academic career but also a spiritual fortune for my future life. I'd say, without his support, everything here at Virginia Tech is impossible.

Next, I thank my committee members, Dr. Jianyong Li and Dr. Iuliana M. Lazar who have provided me with valuable suggestions and comments on my research and the presentation of this thesis.

I also thank our group members, Yan Fu, Dr. Ping Wang, Hang Zhang, Dr. Zhanghan Wu and Philip Hochendoner for their interesting discussion and techniques help on my thesis project. Especially, Yan Fu has helped a lot to teach me (as originally an experimentalist) these computational skills used in this research.

Last but not least, I am grateful to Dennie Munson, Dr. David Bevan, Sue Rasmussen and Dr. Brenda Winkel for all what they have done to help me transfer from GBCB to M.S program in the department of Biological Sciences.

Table of Contents

List of Figures

List of Tables

List of Abbreviations

IFN-γ, interferon-gamma; IL-1, interleukin-1; IL-6, interleukin-6; TNF-α, tumor necrosis factor-alpha; Jak, Janus Kinase; STAT, Signal Transducers and Activators of Transcription; MHC, Major histocompatibility complex; IRF, interferon regulatory factor; IFNGR, interferon-gamma receptor; SH2, Src homology 2; SOCS, suppressor of cytokine signaling; LPS, lipopolysaccharide; LD, low dose; HD, high dose; IP-10, interferon gamma-induced protein 10; TLR4, Toll-like receptor 4; AI, activator induction; PS, pathway synergy; SD, suppressor deactivation; IL-6, interleukin-6; IL-15, interleukin-15; STAT1*D, phosphorylated STAT1 dimer; PPX, unidentified phosphatase in the cytoplasm; PPN, nuclear phosphatase; SHP-2, SH2 domain-containing tyrosine phosphatase 2; IFNR, interferon-γ receptor; RJ, IFNR-Jak complex; IFNRJ, IFN-γ-IFNR-Jak complex; IFNRJ2, IFN-γ-IFNR-Jak complex dimer; IFNRJ2*, IFN-γ-IFNR-Jak complex phosphorylated dimer; STAT1c, cytoplasmic STAT1; STAT1n, nuclear STAT1; STAT1c*, phosphorylated cytoplasmic STAT1; STAT1n*, phosphorylated nuclear STAT1; STAT1n*Dn, phosphorylated nuclear STAT1 dimer; STAT1n*Dc, phosphorylated cytoplasmic STAT1 dimer.

Attribution

Jianhua Xing designed the project; Xiaoshan Jiang, Yan Fu, Hang Zhang and Jianhua Xing performed the computational modeling; Xiaoshan Jiang, Yan Fu and Jianhua Xing wrote the manuscript.

Chapter 1

Introduction and Literature Review

a. Introduction

The beauty and mystery of life partially originate from its complexity but perfection far beyond human being's imagination so that many scientists are trapped in the debate between God's creation and Darwin's evolution. It is also this perfection that leads people into troubles whenever any disorder goes out of certain range tolerable by the life system. The macrophage mediated innate and adaptive immunity is such an example of well-orchestrated and complicated biological process that may cause various diseases after being impaired. In real biological organisms, such as the human body, macrophages are constantly exposed to different pathogens or microbes and respond accordingly to protect us from infection. So it is appealing to decode the seemingly complicacy and unpredictability of macrophage behaviors under different single dose or repetitive doses. Previous research on macrophages is mostly carried out focusing on individual molecule or protein by traditional cellular and biochemistry experimental techniques which could only provide limited information, thus it is unrealistic to understand the whole regulatory network underlying macrophage activities. Recently, microarray as a high through-put technique has been introduced to do the transcriptome profiling of macrophages treated by certain stimulus. It outputs the expression behaviors of thousands of genes at the same time. We believe that through analyzing that information, one can better understand the mechanisms that are responsible for macrophages activation. In addition, systematic biologists and biophysicists have applied mathematical models to simulate the biological system. This provides us a novel

insight into investigating these huge cellular networks and a guideline for performing further experiments to confirm proposed mechanisms.

In this research, we are specifically interested in the interferon-gamma (IFN-γ) priming effect during macrophages activation. The priming effect basically means a dramatically enhanced cellular response after a cell being treated with two subsequent stimuli. In 2005, Hu used microarray to profile all genes that response to single or repetitive IFN-γ stimulation. We hope to build up a pipeline to analyze such microarray data therefore to find potential candidates that may be involved in the priming effect. Also, we form a mathematical model to further investigate the mechanism of IFN-γ mediated priming effect.

b. Macrophage and IFN-γ

Macrophages develop from bone marrow when monocytes leave from blood and enter lymphoid and non-lymphoid tissues [1]. They have originally been defined as an important immune cell that participates in both innate and adaptive immunity response in vertebrate animals. As the first line of defense against pathogen attack, the macrophage is responsible for recognizing infections, up-taking and killing microbes by phagocytosis (Figure 1.1A). During this process, macrophages engulf and digest pathogens or foreign substances [2]. On the other hand, upon antigen invasion, macrophages can be induced to produce various cytokines, including interleukin-1 (IL-1), interleukin-6 (IL-6) and Tumor Necrosis Factor-alpha (TNF-α), which also take part in the non-specific host defense by initiating inflammatory reactions [3, 4]. As for adaptive immune response, macrophages are widely known for their pivotal roles in antigens presentation that they engulf and digest invading microbes; then a specific peptide (called antigen) derived from the microbe is processed to be presented on the major

histocompatibility complex class II (MHC-II) molecules on macrophages surface which is subsequently recognized by T lymphocyte, resulting in T cells activation (Figure 1.1B) [5].

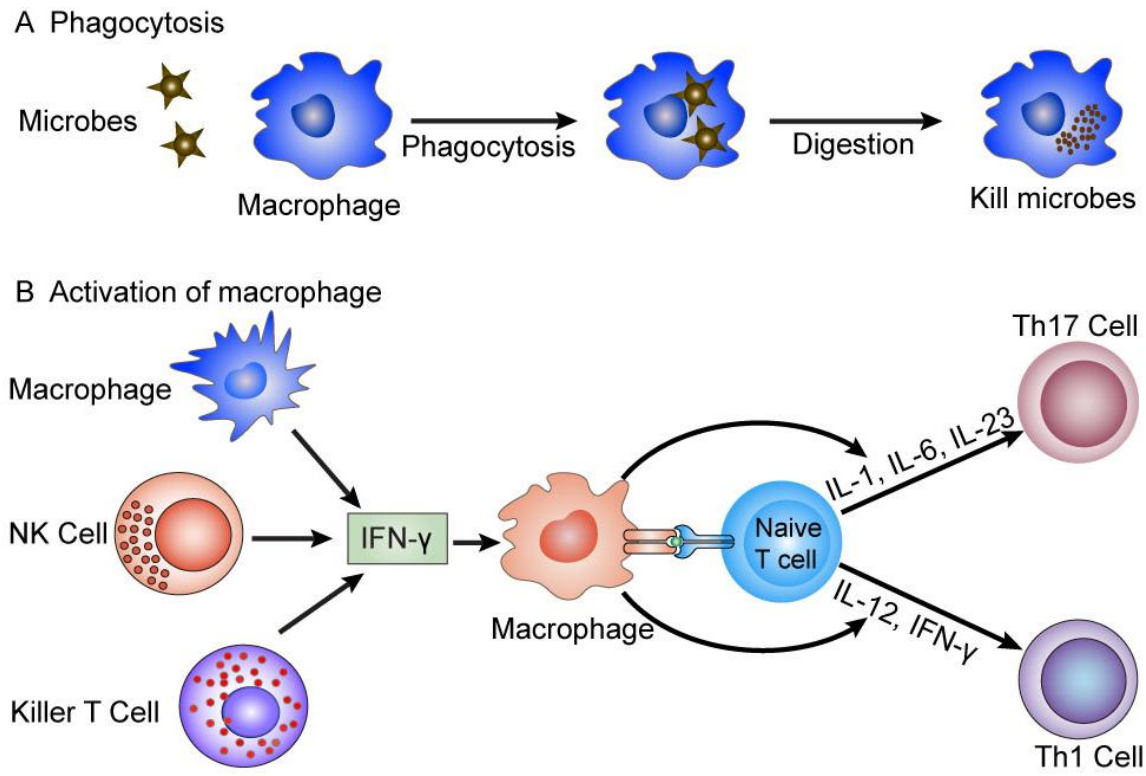

Figure 1.1 Macrophages participate in both innate and adaptive immunity (Adapted from[6, 7]). (A) The macrophage engulfs and digests pathogens or bacteria through a process called phagocytosis. (B) IFN-γ is produced by various cells and it activates macrophage, which further induces na ïve T cells to differentiate into different subgroups.

Activated T lymphocytes are vigorously involved in cell mediated immunity by secreting numerous cytokines, including IL-4, IL-5, IL-17, IFN-γ, etc. [8]. Recently, macrophages have also been reported as a versatile cell that plays important roles in homeostasis, such as would healing, tissue repair and remodeling [6, 9]. Many human diseases, such as rheumatoid arthritis, atherosclerosis and even cancer, have been found to be associated with failure of macrophages'

functions in both immune system and homeostasis. This is becoming one of the most interesting research areas in recent few years [9, 10].

Except for being secreted by T lymphocytes, IFN-γ is also produced by natural killer cells and killer T cells during the early innate immune response (Figure 1.1B) [11, 12]. IFN-γ is the only Type II interferon found in human [13]. It is best described for its crucial ability against viruses and intracellular bacteria or parasites infection by directly interfering viral replication or even destroying the infected host cells via promoting apoptosis [11]. In addition, IFN-γ is able to activate or prime other immune cells, e.g. macrophage, NK cell, resulting in more cytokine production and enhanced pathogen clearance. The canonical signaling pathway that IFN-γ employs to activate macrophage is Janus kinase (JAK)-signal transducer and activator of transcription (STAT) and this activation process is almost indispensable for inflammatory and antimicrobial response [14, 15]. Another vital manner of IFN-γ engaging in infection control is to increase gene expression of some cellular surface molecules, such as MHC I and MHC II on various antigen presenting cells [16, 17]. Up-regulated MHC I and MHC II expression accelerates the presentation of viral peptides to cytotoxic T cells therefore contributing to rapid antigen recognition and breaking-down of infected cells. The activated T helper cells reciprocally stimulate activation of other cells that lead to more cytokine production and initiate stronger adaptive immune response. Any dysregulated IFN-γ production or dysfunction can have a severe impact on human immune system. Many human auto-inflammatory and autoimmune diseases, such as systemic lupus erythematous, multiple sclerosis and diabetes mellitus are related with abnormal behavior of IFN-γ [11]. Last by not least, IFN-γ was even reported to be engaged in preventing tumor development [18]. This is actually achieved by strengthening the immunogenicity of tumor cells and evoking the immune response against transformed cells [11].

c. Jak/STATs pathway

Janus Kinase-Signal Transducer and Activator of Transcription pathway is an evolutionarily conserved signaling pathway that presents in a variety of cells. It is a crucial transduction mechanism to sense a broad array of extracellular signals such as cytokines, chemokines, and growth factors and eventually to promote DNA transcription or repression in nucleus [13]. Jaks are receptor pre-associated protein tyrosine kinases (and there are four mammalian Jaks identified: Jak1, Jak2, Jak3, and Tyk2) while STATs are transcriptional factors (Figure 1.2) [13]. Currently, 7 different members of mammalian STAT family have been identified and they perform a wide range of biological functions, including cell proliferation, differentiation, cell migration, apoptosis as well as viral infection suppression and inflammation [19-21]. Among these STAT members, STAT1 has been well studied as the paradigm of Jak/STAT pathway activated by either type I (IFN-α and IFN-β) or type II (IFN-γ) interferon. STAT1 mediated IFNs signaling is playing a crucial role in modulating immune response of host cells to pathogen invasion by inducing many anti-viral effectors and inflammatory genes such as complements, interferon regulatory factors (IRFs), co-stimulatory molecules, nitric oxide synthases, etc.[13]. Aberrant STAT1 function may cause inefficiency in handling infections with intracellular pathogens [13]. On the other hand, STAT1 has been reported to restrain inflammation thus to avoid excessive immune cell activation and autoimmunity [13]. This contrary yet co-existed role of STAT1 demonstrates a good example of fine-tuned biological mechanism in maintaining homeostasis. During macrophage activation, Jak/STAT pathway is the key player to mediate IFN-γ signaling through membrane bounded IFN-γ receptors, IFNGR1 and IFNGR2.

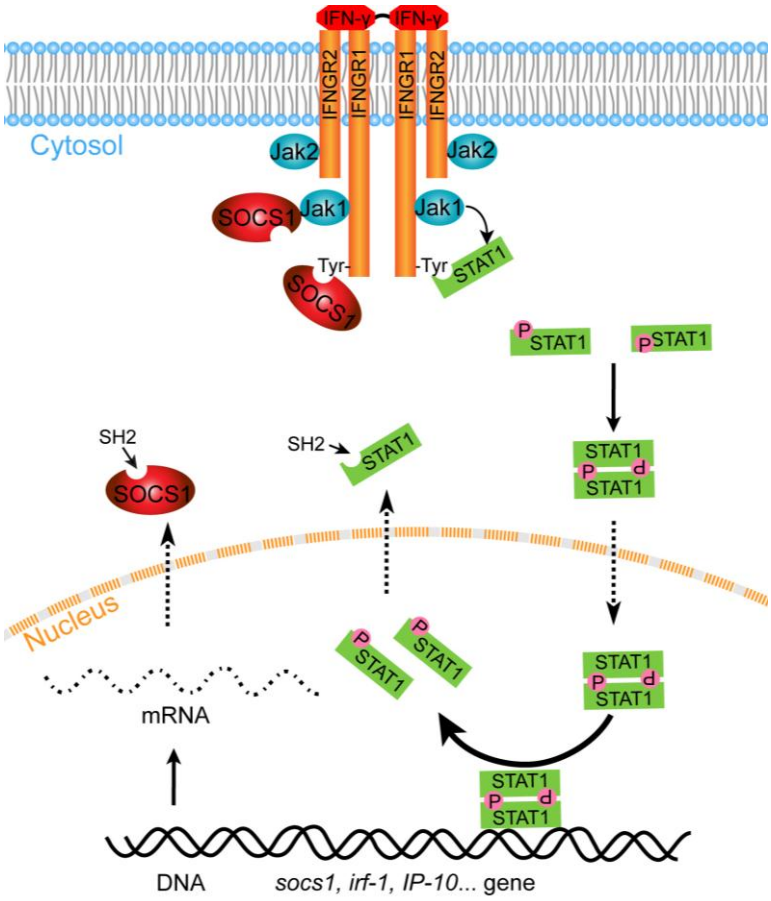

Figure 1.2 The activation and inhibition of Jak/STAT pathway in the macrophage

Upon binding of IFN-γ to its receptors, IFNGR1/2, the two subunits migrate laterally and join together as heterodimers, thus resulting in increased local Jaks concentration and their trans-phosphorylation (Figure 1.2) [20]. Activated Jaks, in turn, initialize the signal transduction cascade by phosphorylating tyrosine motifs present on the cytoplasmic domains of IFN-γ receptors which serve as the docking sites for cytosolic molecules bearing Src Homology 2 (SH2) domains, such as STAT1 and SOCS1 [13]. After STAT1 is recruited to IFNGR1/2 cytoplasmic docking sites via its SH2 domain, it is subsequently phosphorylated by Jaks and then released into cytosol as activated monomers which further assemble into STAT1:STAT1 dimers in a parallel manner (Figure 1.2) [21]. Phosphorylated STAT1 dimers translocate into the

nucleus where they bind to the regulatory DNA elements termed gamma-activated sequence (GAS) and turn on the transcription of downstream genes [21]. As an important transcription factor, STAT1, after being activated, switches on expression of a number of genes including IRF-1, interferon gamma-induced protein 10 (IP10), SOCS3, SOCS1, chemokine receptor 2 (CCR2), etc. It's worthy to note that SOCS1 protein has a profound interference on Jak/STAT pathway activity [22, 23]. SOCS, Suppressor of Cytokine signaling, consists of a family of members that negatively regulate Jak/STAT signaling pathway by targeting Janus kinase protein for proteasomal degradation (Figure 1.2) [23, 24]. Especially, SOCS1 and SOCS3, they both contain a kinase inhibitory region and SH2 domain which enable them to bind to Jaks to inhibit their kinase activity or bind to IFN-γ receptor cytoplasmic docking sites as pseudo-substrates; in either way, they block STAT1 from phosphorylation [24]. This negative feedback is indispensable as it helps dampen Jak/STAT modulated immune activity to avoid autoimmune or tissue damage caused by over active inflammation irritated by IFN-γ.

d. IFN-γ Priming effect

In a paper published on *Nature Immunology* in 2002, it was reported that low dose of IFN-γ treatment was able to sensitize Jak/STAT1 pathway during macrophage activation [25]. In other words, the first sub-threshold IFN-γ stimulation may prime or prepare macrophages for activation by the second dose of IFN-γ. As shown in Figure 1.3A, when given only single high dose of IFN-γ stimulation, macrophages can reach just limited activity in terms of phosphorylated STAT1 dimer; however, if macrophages were pretreated with a low dose of IFN-γ (e.g. 0.15μg/L) for 3 days first, they may achieve a highly increased activity upon the second higher dose of IFN-γ stimulation. This phenomena is called sensitization or priming effect, which defines that cells may achieve largely upgraded response (e.g. cytokine production, gene

expression or activities of certain transcriptional factors in macrophage) under repetitive stimuli that is not just the addition of two responses under individual stimulus (Figure 1.3B).

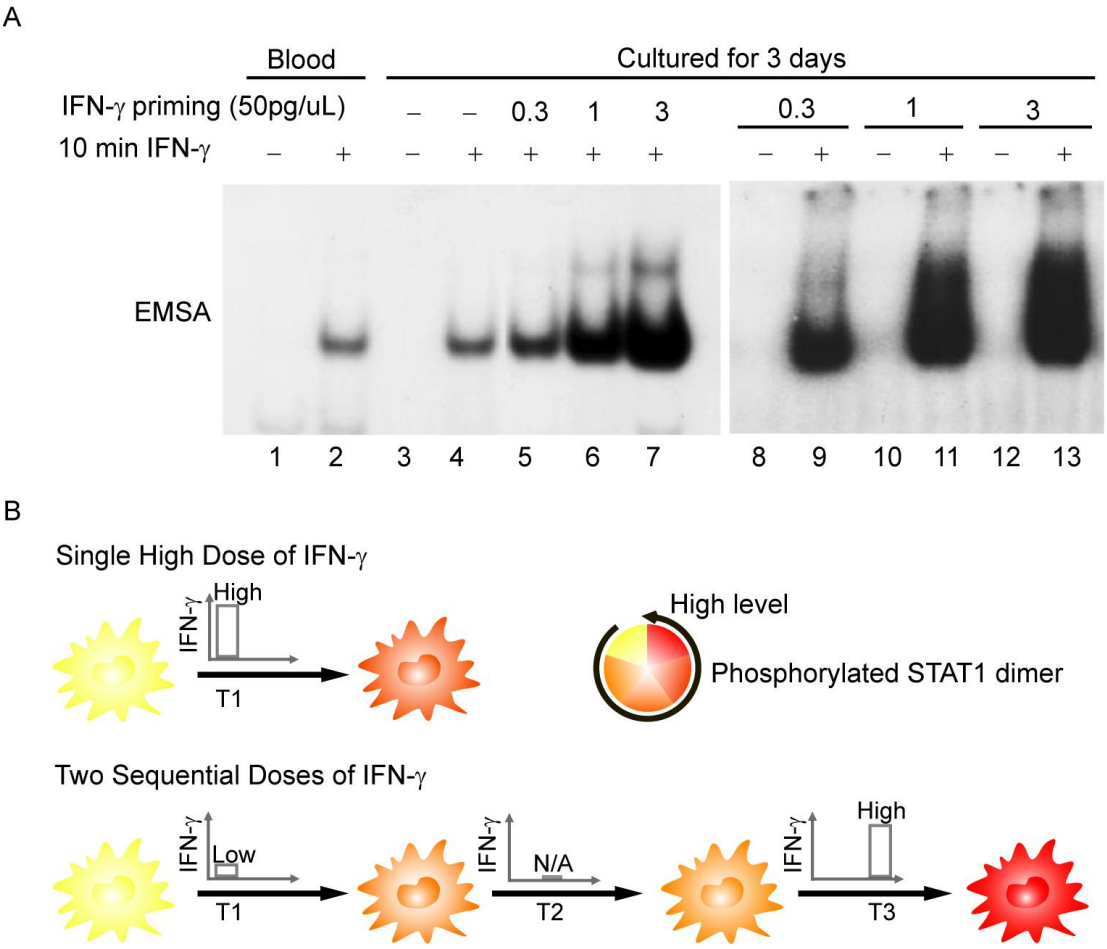

Figure 1.3 IFN-γ mediated priming effect during macrophage activation (A) Experimentally observed IFN-γ priming effect during macrophages activation (adapted from [25]). (B) When a cell is given a single high dose of stimulus, it has a certain level of response; but if the cell is primed with a lower dose first, and followed with a second higher dose, it may achieve a much higher response that is not simply the sum of two responses under each individual stimulus. T1 and T2 and T3 represent different time points.

The molecular mechanisms of IFN-γ-mediated priming effect has been investigated experimentally by Hu et al., who reasoned that an elevated expression of STAT1 by low dose pretreatment was responsible for the induction of priming effect in response to the second high dose of IFN-γ [25]. Low dose IFN-γ exposure does not really activate macrophage; instead, it temporarily switches on the expression of STAT1 but only weakly activates SOCS1, the short half-life inhibitor that decays quickly after expression, hence resulting in a transient accumulation of STAT1 protein [26]. Therefore, the second high dose of IFN-γ can rapidly evoke Jak/STAT pathway, leading to STAT1 phosphorylation which then greatly enhances the expression of many downstream genes, such as SOCS1, IRF-1 and IP-10 [25].

e. Mathematical modeling

Mathematical modeling as a standard approach to study biological problems has been widely used by computational biologists or biophysicists. Briefly, we consider biology in a math perspective and translate biological processes into ordinary differential equations. When building models, genes or gene products are represented by different variables while complicated molecular interactions are described by various parameters. Therefore instead of doing actual experiments with cells or chemical reagents, we use these math equations to simulate the biology system of interest. During the past years, several widely used models, such as mass-action kinetics, hill function and hyperbolic tangent function, are well established and applied to biology research. Based on individual pattern of each system, these models can be modified to describe many specific biological networks that one is investigating. After appropriate parameters being chosen, the model should be able to reproduce the observed experimental data and represent the *in vivo* biological context. Mathematical modeling is a more efficient and time-

saving way to explore biological problems and is capable of guiding experimental design for experimentalists.

Chapter 2

A strategy to study pathway cross-talks of cells under repetitive exposure to stimuli

(Manuscript in preparation)

a. Abstract

Cells are subject to fluctuating and multiple stimuli in their natural environment. The signaling pathways often crosstalk to each other and give rise to complex nonlinear dynamics. Specifically, repetitive exposure of a cell to a same stimulus sometime leads to augmented cellular responses. Examples are amplified pro-inflammatory responses of innate immune cells pretreated with a sub-threshold then a high dose of endotoxin or cytokine stimulation. This phenomenon, called priming effect in the literature, has important pathological and clinical significances. In a previous study, we enumerated possible mechanisms for priming using a three-node network model. The analysis uncovered three mechanisms. Based on the results, in this work we developed a straightforward procedure to identify molecular candidates contributing to the priming effect and the corresponding mechanisms. The procedure involves time course measurements, e.g., gene expression levels, or protein activities under low, high, and low + high dose of stimulant, then computational analysis of the dynamics patterns, and identification of functional roles in the context of the regulatory network. We applied the procedure to a set of published microarray data on interferon-γ mediated priming effect in human macrophages and identified a number of network motifs that possibly contribute to interferon-γ priming. Moreover, a further detailed mathematical model analysis further reveals how combination of different mechanisms leads to the priming effect. One may perform systematic screening using the proposed procedure combining with high throughput measurements, at both transcriptome and proteome levels. It is applicable to various priming phenomena.

b. Introduction

A cell needs to constantly sense and response to various signals from both external and internal environments. The requirement on generating appropriate response to specific signals forces cells to develop a complex signaling network that often involves multiple highly intertwined signaling pathways [27-29]. It becomes increasingly clear that pathway cross-talks play critical roles in cellular signaling and decision making process [30]. For example, cross-talks may increase the nonlinearity in the signaling network, resulting in various synergistic and antagonistic effects in cellular responses [31-34]. A nonlinear response refers to the cellular response to multiple different stimuli, or repetitive stimulus that is not simply the sum of responses to each individual stimulus. Cells in vivo are constantly exposed to a variety of stimulus with fluctuating concentration. Therefore it is of great importance to study how cells utilize complex pathway cross-talks to generate appropriate response or make correct decision to multiple or repetitive stimulus. Pharmaceutically, it is also a common treatment strategy to use combinations of multiple drugs simultaneously in order to generate synergistic effect [34, 35]. Therefore, the nonlinear phenomena due to pathway cross-talks have important physiological and clinical significances.

In this work we focus on cellular priming effect (also called preconditioning and sensitization) which refers to a well-observed phenomenon that after being treated with a seemingly negligible concentration of stimulus, a cell may achieve amplified responses upon a second exposure to the same stimulus at higher concentration [25, 36, 37]. The priming effect reflects the nonlinear nature of the system because the cellular response to repetitive stimuli is stronger than the sum of that to individual low and high dose stimulation. Since the cellular response to the low dose stimulation is negligible, in experimental practice one usually

approximates the above sum by the cellular response under the high dose stimulation alone. Two such examples are lipopolysaccharide-mediated (LPS) and Interferon-γ-mediated (IFN-γ) priming effects observed in innate immune cells such as monocytes and macrophages [25, 38]. For example, LPS is the pathogen-associated molecular pattern (PAMP) expressed on the outer membrane of gram-negative bacteria. Several in vitro studies have reported that low dose LPS (e.g. 0.05-1 μg/L) can prime macrophages for an augmented pro-inflammatory cytokine production under high dose LPS (10-100 μg/L) [36-40]. Clinically, evidence relates this LPS-mediated priming phenomenon to low-grade metabolic endotoxemia, which is defined as an elevated but physiological LPS concentration in the blood, resulting in a higher incidence of insulin resistance, diabetes and atherosclerosis [41-46]. Similarly, a sub-activating dose of IFN-γ (e.g. 0.05-0.15 μg/L) is able to prime macrophages for an enhanced activity of signal transducer and activator of transcription 1 (STAT1) under an activating dose of IFN-γ (e.g.0.5-5 μg/L) (Figure 1.3). As a consequence, the expression of a number of genes regulated by STAT1 are also increased, including IFN regulatory factor 1 (IRF-1) and inducible protein-10 (IP-10). Since IFN-γ plays a crucial role in interfering viral replications and promoting apoptosis of infected cells, abnormality in IFN-γ production can lead to severe consequences in the immune system [11]. The sensitization of IFN-γ signaling also correlates with several immune system malfunctions and diseases, such as rheumatoid arthritis, hepatitis and multiple sclerosis [11, 26, 47]. Hu et al. first investigated the molecular mechanisms of IFN-γ-mediated priming effect and reasoned that an elevated expression of STAT1 by low dose pretreatment was responsible for the induction of priming effect [25]. However, other molecular mechanisms may also exist.

In the previous study, Computational analysis has been applied to enumerate all possible network motifs that are able to induce priming effect in a generic three-node regulatory network.

Strikingly, it was found that the *in silico* discovered priming motifs naturally fall into three priming mechanisms[48]. Based on the finding, the main purpose of this study is to design and apply a general combined experiment and computation strategy to search for molecular candidates contributing to the priming effect for a given stimulus. The remaining part of the paper is organized as follows. First we summarize the main results of previous study, and outline the strategy. Then we demonstrate how to apply the strategy to analyze a set of published microarray data on IFN-γ-mediated priming effect. Next we show further analysis on a detailed ordinary differential equation based model.

c. Results and Discussion

Computational analysis suggests basic priming mechanisms

Previously, all possible network structures and kinetics that are able to induce priming effect have been enumerated by simplifying these intracellular interplaying signaling pathways into a generic three-node model [48]. The three-node model represents the minimal abstraction of the two cross-talking pathways (e.g., MyD88-dependent and -independent branches of Toll-like receptor 4 (TLR4) signaling pathway). As shown in Figure 2.1A, x_1 and x_2 represent two interacting pathways, x_3 is where these two pathways converge with each other and serves as the readout to show the priming effect (x_1, x_2 and x_3 may also simply stands for three different genes or proteins). Each node in the model can either positively or negatively regulate the activity of the other nodes or itself. We simulated the dynamics with a set of nonlinear ordinary differential equations with 14 variable parameters. Through a two-stage Metropolis algorithm, we analyzed the dynamical behavior of over 1.5×10^5 different networks that can generate priming effect [48]. Here we refer to priming effect as a set of dose-response behaviors: (1) A single low dose

stimulant (LD) cannot activate the readout x_3 (< 0.1 in a reduced unit with 1 the maximum induction). (2) A single high dose stimulant (HD) can activate x_3. (3) Sequential stimulation with LD first followed by HD (LD+HD) can activate x_3 to a maximum level that is at least 50% higher than that under HD alone.

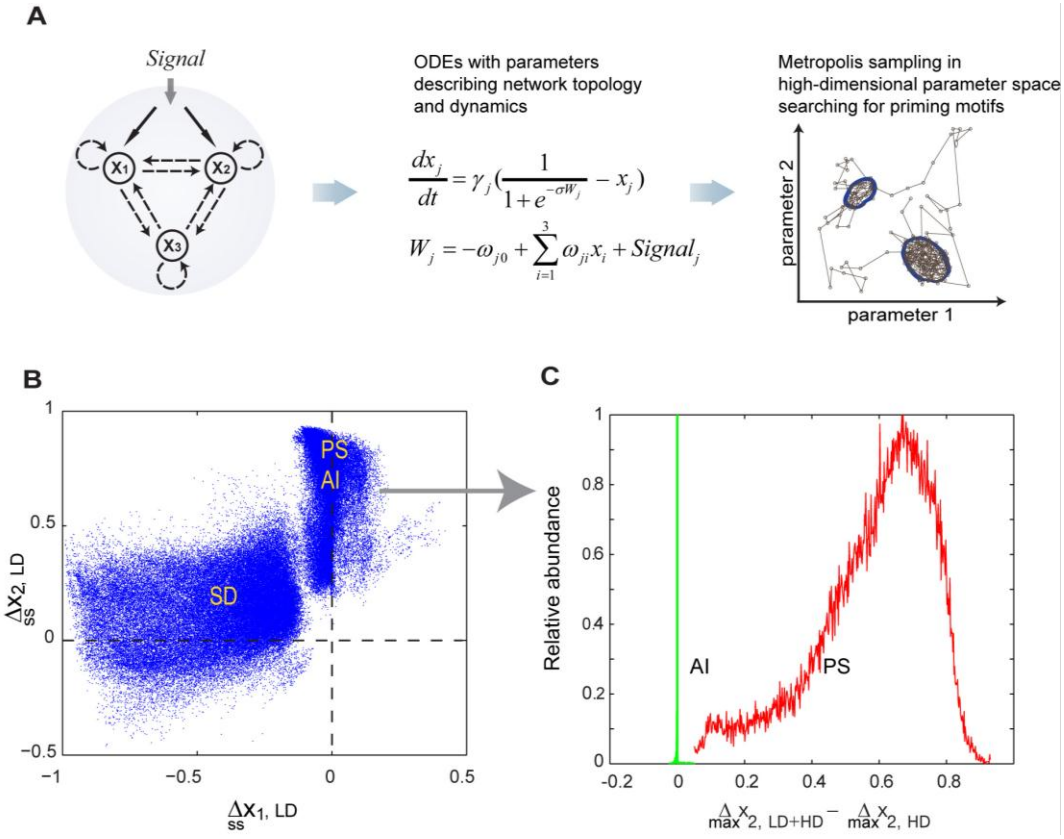

Figure 2.1 Summary of theoretical analysis[48] (A) An abstract three-node model was chosen to represent that the stimulus can activate two parallel pathways (through x_1 and x_2) which converge to the monitored readout (x_3). A set of corresponding ordinary differential equations (ODEs) were constructed, and a Metropolis sampling algorithm was used to search for parameter sets giving the priming effect in the high-dimensional parameter space. (B) Computational studies show that the parameter sets leading to priming naturally divide into two regions, corresponding to different priming mechanisms. $\Delta_{ss} x_{1,LD}$ ($\Delta_{ss} x_{2,LD}$): change of x_1 (x_2) level at the

end of LD treatment period compared to those of untreated cells. (C) The right region in B can be further discriminated according to the sample abundance distribution (relative to the maximum within each group) of $\underset{\max}{\Delta} x_{2,LD+HD} - \underset{\max}{\Delta} x_{2,LD}$ (difference between the maximum level of x_2 during the HD treatment period after LD pretreatment and that of x_2 without LD pretreatment), suggesting overall three priming mechanisms. Panels A is adapted from [48].

As shown in Figure 2.1B, the parameter sets leading to priming effect clearly cluster into two regions, in terms of the change in the two regulators, x_1 and x_2, at the end of LD pretreatment ($\underset{ss}{\Delta} x_{i,LD}$, i=1,2). Data in the left region locate approximately along the negative side of x-axis, that is, a LD pretreatment decreases x_1 in this region (i.e. $\underset{ss}{\Delta} x_{1,LD} < -\delta < 0$, with an arbitrarily chosen cutoff $\delta = 0.1$ to account for possible experimental resolution). Notice x_2 in this region spread out vertically, that is, x_2 can either increase or decrease to some extent under LD pretreatment. Based on this observation, we want to find out any possible constraint on x_2 in this region. To do this, we plotted the distribution of the change in the maximum response of x_2 between under LD+HD and under HD alone. As shown in Figure S1, we found that x_2 from this region can be either HD-responsive or LD-responsive, but with a constraint that the maximum expression under LD+HD makes no difference with that under HD alone (i.e. $\underset{\max}{\Delta} x_{2,LD+HD} \approx \underset{\max}{\Delta} x_{2,HD}$) (Figure S1). On the other hand, the data in the right region demonstrate a significant increase in x_2, but not x_1, after LD pretreatment (Figure 2.1B) (i.e. $\underset{ss}{\Delta} x_{2,LD} > \delta$). The maximum expression of x_1 under LD+HD makes no difference with that under HD alone (i.e. $\underset{\max}{\Delta} x_{1,LD+HD} \approx \underset{\max}{\Delta} x_{1,HD}$) (Figure S1). However, this overlapped region can be further separated into two sub-groups, pathway synergy (PS) and activator induction (AI) if plotted

against another experimentally measurable quantity- the difference in the maximum level of x_2 under LD+HD *vs* under HD (Figure 2.1C). To illustrate, it is obvious that the data from the red group, but not the green group, shows a significant increase in the maximum level of x_2 under LD+HD compared to that under HD alone (i.e. $\underset{\max}{\Delta} x_{2,LD+HD} - \underset{\max}{\Delta} x_{2,HD} > 0$) (Figure 2.1C).

Further statistical analysis on network topologies reveals that data from each priming group shares a unique network structure (Figure 2.2, left column). For example, x_1 in the left region in Figure 2.1B is identified as an inhibitor to the readout x_3. Since x_1 is decreased by LD, we therefore named this region "Suppressor Deactivation" (SD). Similarly, x_2 in right region in Figure 2.1B is found to be an activator to x_3. Based on the fact that the data in this region can be further differentiated in terms of differential dose-response $\underset{\max}{\Delta} x_{2,LD+HD} - \underset{\max}{\Delta} x_{2,HD}$, we further named them "Pathway Synergy" (PS, denoted in red) and "Activator Induction" (AI, denoted in green), respectively (Figure 2.1C).

The physics underlying the three priming mechanisms turns out to be simple and beyond the current three-node model [48]. For Pathway Synergy, both of the two pathways activate the priming readout x_3, but one has a fast time scale and a high activation threshold while another one has a slow time scale and a low activation threshold. When given a single HD stimulation, the regulation on x_3 from the two pathways is temporally separated. A LD pretreatment brings forward the slow pathway so that the two pathways can achieve a transient synergy to boost the production of x_3 (Figure 2.2). Similarly, for Activator Induction and Suppressor Deactivation, a LD pretreatment separates the two originally temporally overlapping but antagonistic pathways by either advancing the activator or delaying the suppressor (Figure 2.2).

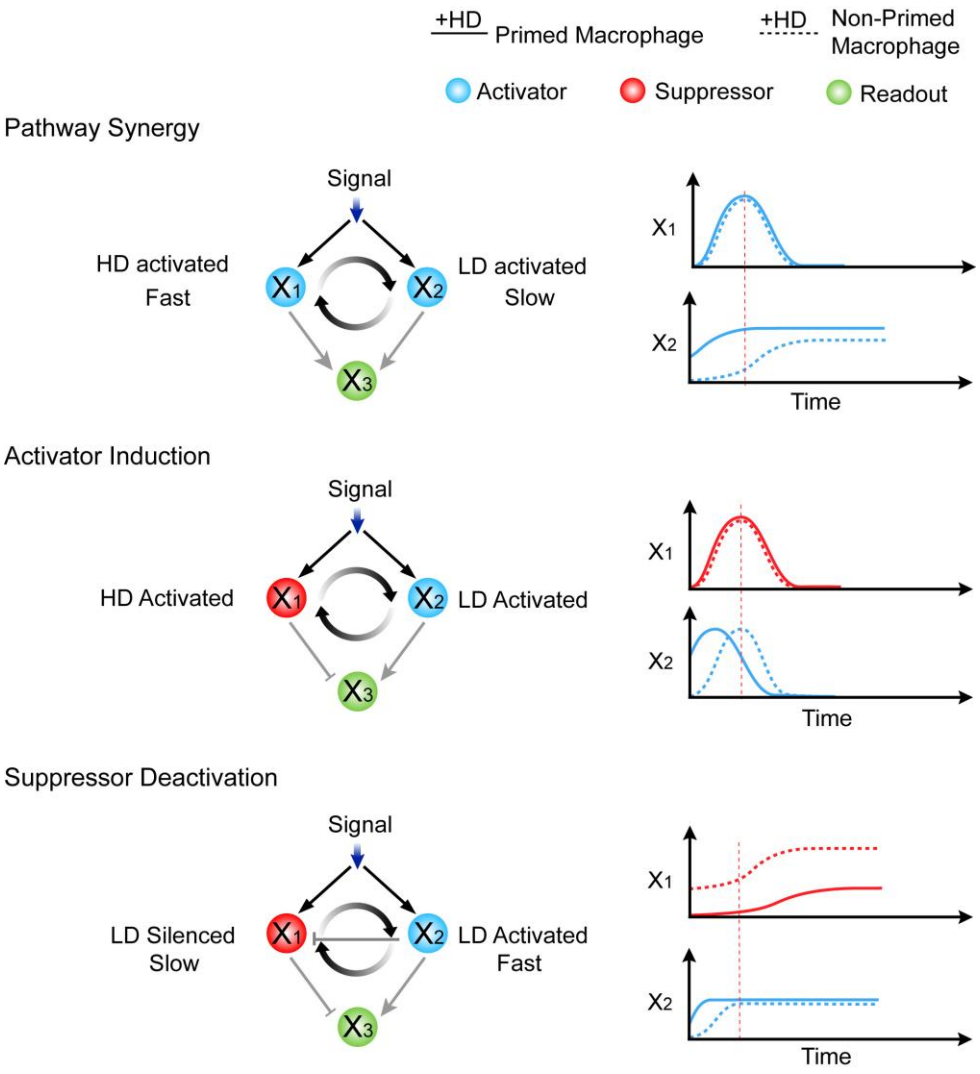

Figure 2.2 Schematic illustrations of the three *in silico* found priming mechanisms The left column shows the basic topological requirement identified in the corresponding priming dataset generated in the theoretical analysis. The right column shows the typical time course of each priming mechanism.

Since each priming mechanism highlights unique topological and dynamical characteristics, we propose that one can utilize this important information to guide microarray analysis on identifying groups of candidate genes that contribute to priming effect. The

computational result in Figure 2.1B and 2.1C actually suggests a simple procedure to this purpose. The analyzing procedure is summarized as follows (also see Figure 2.3):

1. Record the time course of the cellular response under single LD, single HD, and LD+HD, respectively.
2. Identify the priming readout genes as those with higher response to LD+HD than HD, but with no significant response to LD.
3. Identify the genes induced or reduced by LD (LD-responsive genes), and those responding to HD only (HD-responsive genes).
4. Construct the interactive networks through integrating the available experimental results, and available databases. Examine the identified genes in the context of the network regulations and identify the corresponding molecular mechanisms for priming they potentially contribute to:
    - Pathway Synergy: (1) LD-responsive genes (with the expression under LD+HD higher than that under HD alone) and (2) HD-responsive genes; (3) both activate a downstream readout gene.
    - Activator Induction: (1) LD-responsive genes (with the expression under LD+HD similar to that under HD alone) and (2) HD-responsive genes; (3) the LD-responsive gene activates while the HD-responsive gene inhibits a downstream readout gene.
    - Suppressor Activation: (1) LD-reduced genes and (2) LD/HD-responsive genes (with the expression under LD+HD similar to that under HD alone); (3) the LD-reduced gene inhibits while the LD/HD-responsive gene activates a downstream readout gene.

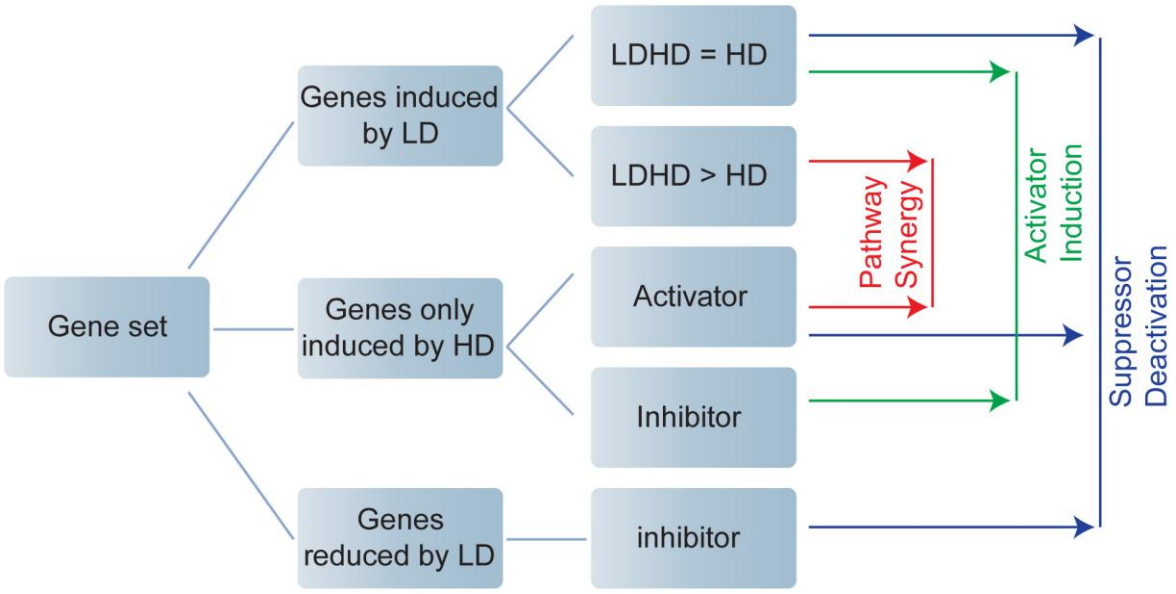

Figure 2.3 Proposed procedure of microarray analysis for identifying candidate genes under different priming mechanism LD: low dose stimulation; HD: high dose stimulation. Second column: Genes are grouped according to their expression behaviors under LD and HD, respectively. Third column: genes are further sub-grouped according to the differential expression under LD+HD or under HD alone. Genes that can only be induced by HD are further differentiated according to their regulatory characteristics (e.g. activator or inhibitor) to the readout gene. Fourth column: combinations of gene from different sub-groups reveal potential priming motifs (x_1 and x_2 in Figure 2.2).

Microarray data analysis predicts possible candidates involved in the induction of IFN-γ-mediated priming effect

In this section, we focus on the microarray data on IFN-γ by Hu et al. [22] in order to demonstrate the proposed analyzing procedure. This is the only set of data we found from the microarray database Gene Expression Omnibus that satisfies the requirement in the above discussed procedure. After two steps of data processing (see Methods for details), we found 225

genes demonstrating non-trivial dynamics (i.e., significantly changed under at least one condition, see Methods for details). They form the subjects of our analysis. Hierarchical clustering of these genes shows that the majority of them do not show statistically significant change (by ≥ 2 fold) under LD (Figure 2.4). However, we found that 27 genes are significantly increased (by ≥ 2 fold) by LD, and 20 significantly decreased (by ≥ 2 fold) by LD (Figure 2.4, the probe names and gene symbols are listed on the right). Based on the proposed analyzing procedure, these genes constitute the candidate regulators for different priming mechanisms (Figure 2.3). These genes will then be subject to further analysis, such as examining them in the context of the regulatory network (discussed later). Moreover, since the level of the LD-responsive regulator in PS mechanism is dramatically increased under LD+HD than under HD alone, while the corresponding regulator in AI barely shows any difference (Figure 2.1C), these 27 LD-responsive genes can be further sub-grouped into either PS or AI category based on their expression profiles accordingly (i.e. $\underset{\max}{\Delta} x_{i,LD+HD} - \underset{\max}{\Delta} x_{i,HD}$).

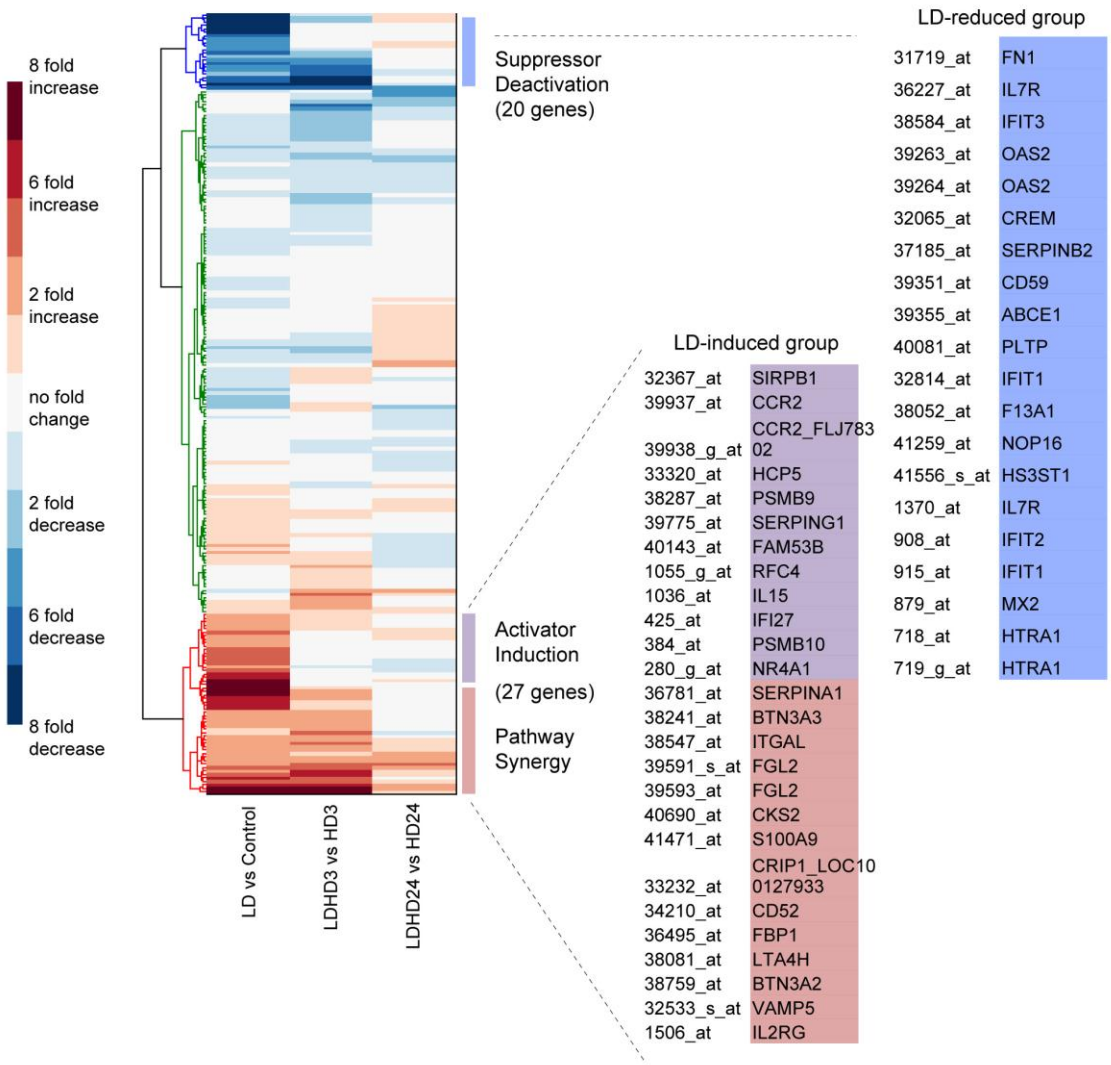

Figure 2.4 Analysis of the microarray data (GEO, accession number: GDS1365) Hierarchical clustering of the gene expression profiles over 225 genes. The left, middle and the right columns denote the fold change under LD *vs* Control, LD+HD *vs* HD (3 hr), and LD+HD *vs* HD (24 hr), respectively. Genes that are statistically increased and decreased by LD are listed on the right. These genes are grouped into different priming mechanisms according to the guideline shown in Figure 2.3.

Other genes that are not responsive to LD stimulation are further clustered according to the gene expression patterns. We found that a large portion of such genes can be activated by HD alone (Figure 2.5). Based on the guidance shown in Figure 2.3, they are potential candidates for the HD-responsive regulator in the three priming mechanisms. In addition, we found that these genes are activated with basically three dynamical patterns: early-, late-, and persistently-responsive dynamics (Figure 2.5). For example, RelA is found only expressed in the HD 3hr group, but not in the HD 24hr group, suggesting an early- dynamics. SOCS1 is found in both HD 3hr and HD 24hr, indicating a persistent dynamics. This dynamical property is also necessary in assembling appropriate genes onto specific priming motifs.

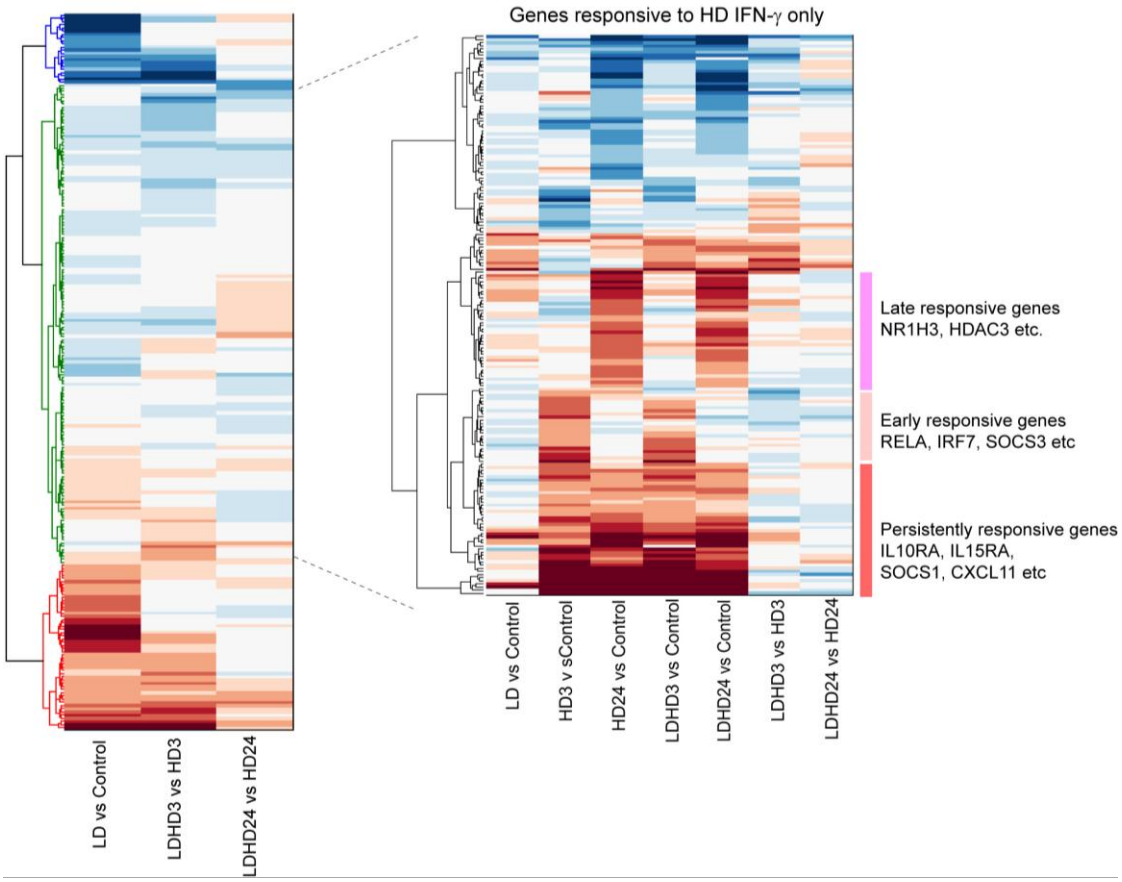

Figure 2.5 A second step hierarchical clustering over the genes that only respond to

HD Gene expression patterns are clustered according to the fold change under LD *vs* Control, HD *vs* Control (3hr), HD *vs* Control (24hr), LD+HD *vs* Control (3hr), LD+HD *vs* Control (24hr), LD+HD *vs* HD (3hr), and LD+HD *vs* HD (24hr). At least three major dynamical groups are identified among genes that are activated by HD stimulation.

Furthermore, five genes (SLC2A3, ST3GAL5, DNAJB1, STAT1, UBE2S) are identified as possible priming readout genes (x3) which show negligible expression under LD, but considerable higher expression under LD+HD than under HD alone. However, among the five genes, only UBE2S shows a significant change between LD+HD and HD (by ≥ 2 fold) that passes *t*-test with $p < 0.05$. Considering microarray data are usually noisy, one needs more quantitative measurements, e.g., real time PCR to confirm these results. Here we used the experimentally confirmed molecular species, such as phosphorylated STAT1 dimer, IRF-1 and IP-10 as the priming readout [25]. After selecting and grouping genes based on the guideline in Figure 2.3, we then placed them in the context of regulatory networks in order to identify possible priming mechanism on the molecular interaction level. The regulatory network associated with these selected genes is constructed in Ingenuity Pathway Analysis (IPA®) database (see Methods for details).

Here we show several potential PS and AI motifs identified from the regulatory network (Figure 2.6). For example, a PS motif (the second motif on the right) composes a HD-induced regulator (TNFα), a LD-induced regulator (S100A9), and a readout (phosphorylated STAT1). The priming effect can be achieved by synergizing the two positive regulators, TNFα and S100A9, to get the STAT1 activity enhanced. This may be explained by the fact that an increased level of S100A9 by IFN-γ pretreatment may be able to activate P38 [54], which further

up-regulates STAT1 activity. An alternative connection between S100A9 and STAT1 activity is through IL-6.

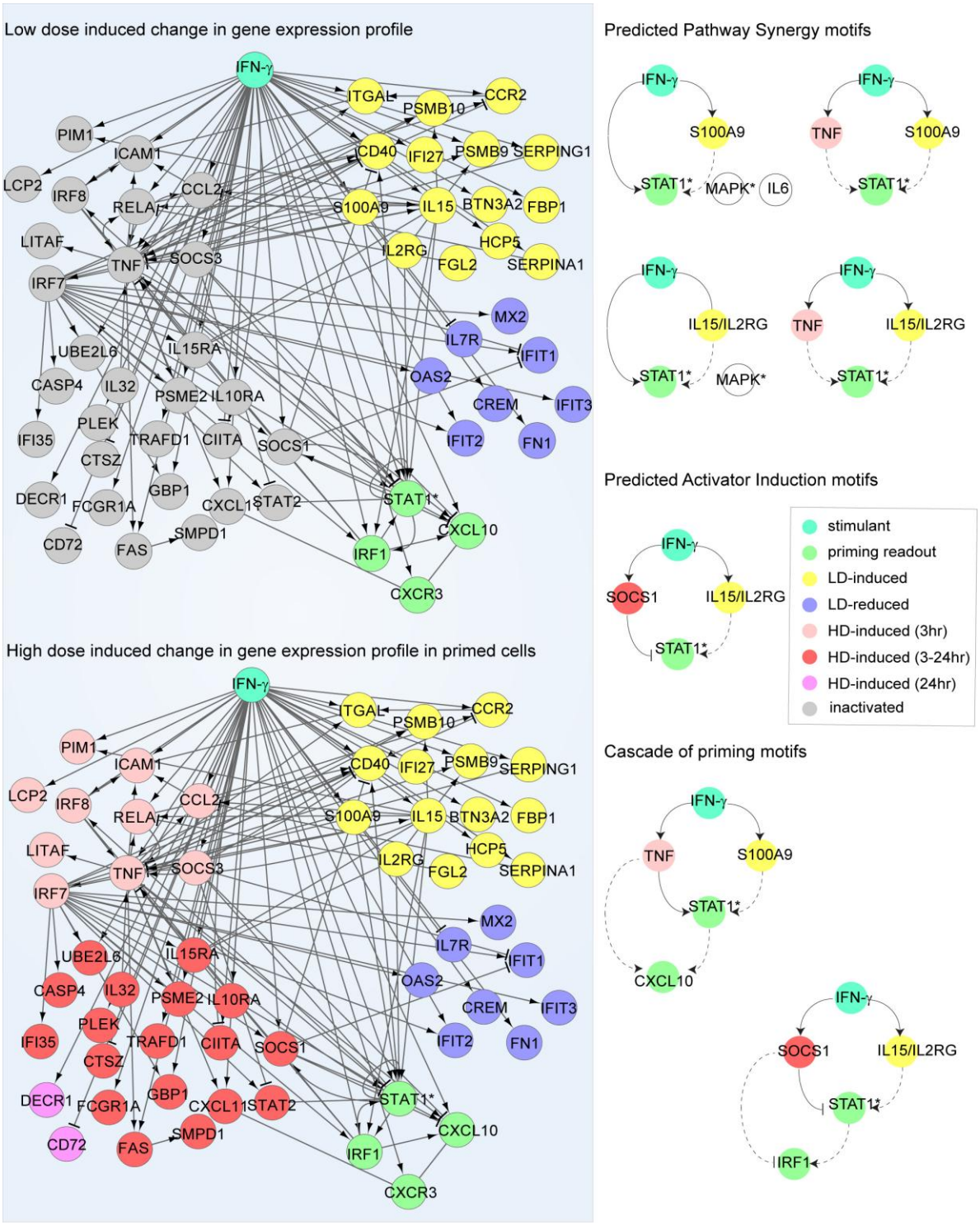

Figure 2.6 Construction of the regulatory networks associated with the selected genes

using IPA® database Left panel: The selected groups of genes with different dose-response and dynamics are put into IPA® database to identify signaling and regulatory relationships with the readout molecules (see Methods for details). Right panel: Priming motifs with different priming mechanisms are identified from the network under the guideline shown in Figure 2.3.

S100A9 has been shown able to trigger IL-6 expression [49], which in turn stimulates STAT1. Therefore an autocrine signaling may also be involved. The true connection should be context dependent, and needs to be confirmed by further experiments. Moreover, a motif that fits in AI mechanism can also be identified from the regulatory network. This AI motif involves interleukin-15 (IL-15) and IL2Rγ as the LD-responsive activator, and SOCS1 as the HD-inhibitor for STAT1 activity. It has been shown that both IL15 and IL2Rγ are able to increase STAT1 activity [50], and from the microarray analysis we show that they can be significantly induced by LD (> 2 fold, $p < 0.05$), while the inhibitory function of SOCS1 against STAT1 is only induced under HD. Therefore, the two counteractive pathways exert AI priming mechanism. As multiple priming motifs are identified on different levels in the regulatory network, we speculate these interconnected priming motifs may work in concert to induce an overall priming effect. A functional redundancy and robustness may also be achieved due to the complex cross-talks brought by these priming motifs in the regulatory network. As a matter of fact, both cascade and parallel layout priming motifs are found in this network (Figure 2.6). Detailed computational modeling can provide great help in understanding the potential functions, advantages and disadvantages brought forth by different combination of the priming motifs.

In our proposed strategy it is essential to examine the genes identified from the high throughput data in the context of the regulatory network. In many cases gene activities are

correlated, e.g., due to a common upper stream regulator. As an illustrative example, suppose the activities of genes A and B are correlated and are both up-regulated by the low dose stimulant, but only A regulates the downstream readout gene C. Based on the absence of regulation from B to C in the regulatory network, one can only conclude that the existing experimental result suggests A, but not B, as a potential contributor to the priming of C. In another situation, if a molecular species (e.g. a transcription factor) shows priming effect, the priming effect may be transmitted to its downstream targets. The detailed model discussed below gives such an example.

Functional clustering further suggest influence of low dose pretreatment on altering cellular functions

To investigate how LD priming affects macrophage cellular functions, we conducted function analysis of the genes that show significant fold change (by≥ 2 fold, p<0.05) after LD priming. Figure S2 shows the clustering result, and lists the top 10 significantly enriched molecular functions found for LD IFN-γ induced and reduced genes, respectively. We found that in general, genes that are significantly increased by LD priming are associated to inflammatory response and immune system process; genes that are significantly decreased are associated to negative regulation of T cell mediated cytotoxicity and immunity. These results suggest that LD priming prepares macrophages for a stronger response through elevating a number of inflammatory genes and inhibiting some negative regulators, reflecting a cellular adaptivity of innate immune cells.

Low dose IFN-γ priming reprograms the gene expression profiles of macrophages

In order to find out whether LD IFN-γ pretreatment could possibly reprogram the gene expression dynamics, we grouped genes based on their induction dynamics under either HD or LD+HD stimulation (e.g. early-, late-, and persistent-response). We found that the number of early response genes increases in primed macrophages (from 78 to 105), while the number of late- and persistent- genes stays almost the same. Strikingly however, the actual composition of genes in each dynamical group has been changed by LD IFN-γ priming (Figure 2.7A). For example, nearly half of the genes from both the early- and the late-response groups are switched off (or show negligible expression) in the primed cells (shown in the red ellipse and the green ellipse that does not overlap with others). Gene Ontology analysis shows that these genes are functionally associated with protein kinase inhibitor activity (the early-response group) and negative regulation of apoptosis (the late response group), indicating a functional change due to the LD pretreatment. Moreover, we also observed a reshuffling of genes among different dynamical groups (Figure 2.7B). For instance, five early-response genes are switched into either the late- or the persistent- response group, while 17 late-response genes are moved into the early- or the persistent-response group, in primed macrophages. Figure 2.7B lists the most significantly enriched gene functions associated to each group of these reshuffled genes. To sum up, the LD IFN-γ priming, to some extent if not globally, is able to reprogram the gene expression profiles by switching genes on and off or changing their expression dynamics.

A

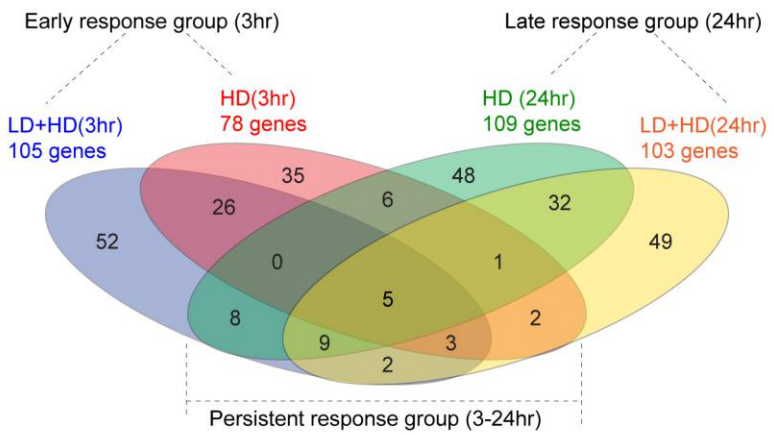

B

HD / LD+HD	Genes	Top enriched GO term
Early response group (3hr) → reshuffle → 2 genes → Late response group (3hr)	35735_at GBP1 39723_at CUL1	cullin-RING ubiquitin ligase complex SCF ubiquitin ligase complex
Early response group (3hr) → reshuffle → 3 genes → Persistent response group (3-24hr)	36629_at TSC22D3 37893_at PTPN2 883_s_at PIM1	transcription factor activity protein tyrosine phosphatase activity
Late response group (24hr) → reshuffle → 8 genes → Early response group (3hr)	36227_at IL7R 36781_at SERPINA1 39119_at IL32 40505_at UBE2L6 36495_at FBP1 38052_at F13A1 40081_at PLTP 41871_at PDPN	blood coagulation
Late response group (24hr) → reshuffle → 9 genes → Persistent response group (3-24hr)	1370_at IL7R 31719_at FN1 32860_g_at STAT1 33916_at NISCH 40639_at SCO2 2058_s_at ITGB5 32207_at MPP1 33339_g_at STAT1 35693_at HPCAL1	thymidine phosphorylase activity IL-7 binding
Persistent response group (3hr) → reshuffle → 0 genes → Early response group (3hr)		
Persistent response group (3hr) → reshuffle → 1 genes → Late response group (24hr)	38066_at NQO1	NAD(P)H dehydrogenase (quinone) activity

Figure 2.7 The gene expression kinetics has been reprogrammed during the low dose IFN-γ priming. (A) Four-way Venn Diagram demonstrated LD IFN-γ pretreatment reprogramed gene

expression profiles of a large number of genes. (B) Kinetic reshuffling in a small number of genes is also identified. The gene name, probe name and the enriched gene ontology are shown in the second and the third column.

Detailed experimental and model study further confirm the analysis result

We want to make it clear that the generic procedure shown in Figure 2.3 is not restricted to microarray data analysis. Microarray is a high throughput technique but less quantitative. One can only detect genes with significant fold change (usually by ≥ 2 fold). For many priming effects, the fold change is less than 2 [36, 38]. Often more quantitative methods such as real time PCR are needed to confirm the microarray findings. Furthermore information on posttranslational and epigenetic modifications requires other techniques. In many applications, it is advantageous to combine time course data under LD, HD, and LD+HD stimulant obtained with different techniques. Here we use one example to illustrate this point.

Our microarray analysis suggested that STAT1 and SOCS1 may participate in a potential priming motif activated by IFN-γ (Figure 2.6), which is in consistence with the experimental observations by Hu et al. [25]. Hu et al. reported that a pretreatment of a sub-threshold IFN-γ sensitized the Jak/STAT signaling for a second dose of IFN-γ [25]. They found that a low dose IFN-γ exposure is able to switch on the transcription of STAT1but only weakly activates the inhibitor SOCS1 in a transient manner [26]. Since STAT1 protein is more stable than SOCS1 protein, the elevated expression of STAT1 actually increased the free available protein molecules for STAT1 docking and phosphorylation in response to the second dose of IFN-γ, thereby contributing to the induction of priming effect.

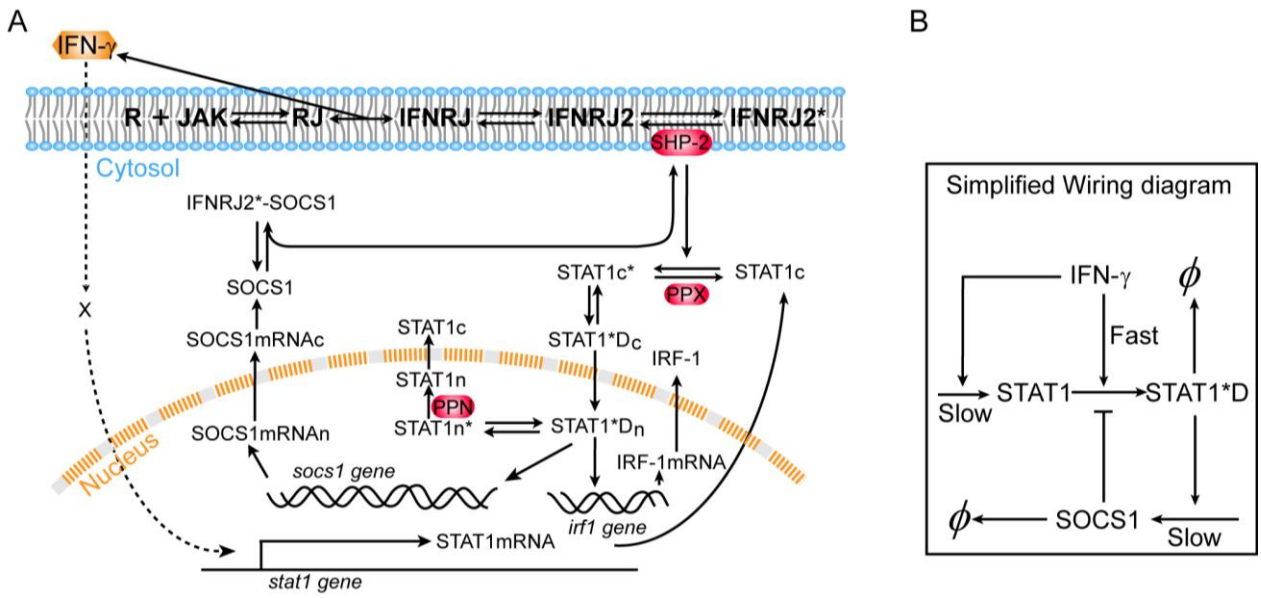

Figure 2.8 Wiring diagram of IFN-γ signal transduction (A) Detailed wiring diagram used in the numerical simulations. IFN-γ binding to the cell membrane embedded Receptor/Jak complex leads to dimerization of the binding complex, and subsequent phosphorylation of Jak molecules; the phosphorylated dimer IFNRJ2* recruits and phosphorylates cytoplasmic STAT1 molecules, which then dimerize and move into the nucleus, functioning as transcription factors to induce expressions of *socs1*, *irf1*, and many other genes; SOCS1 can either bind to Jak and inhibit its activity or compete with STAT1 on binding to IFNRJ2*. IFN-γ also induces *stat1* expression through an unknown mechanism independent of the Jak-STAT canonical pathway. Here we use "X" to represent the undetermined intermediate that senses IFN- γ and regulate *stat1* transcription. For the molecular species, "c" and "n" refer to cytoplasm and nucleus, respectively; "*" refers to phosphorylation. This diagram is adapted from [51]. (B) A simplified wiring diagram to emphasize the three key processes with different time scales contributing to the priming effect.

To further analyze the mechanism, we performed computational analysis using an ordinary differential equations (ODEs) model. The wiring diagram in Figure 2.8A summarizes all the relevant biochemical events in the IFN-γ signaling pathway. A HD IFN-γ can rapidly evoke Jak/STAT pathway, resulting in STAT1 phosphorylation which then induces the expression of many downstream gene, such as SOCS1, IRF-1 and IP-10 [25]. SOCS1 contains a kinase inhibitory region and Src homology 2 (SH2) domain [52]. It binds to Jak to inhibit its kinase activity, or alternatively it binds to IFN-γ receptor cytoplasmic docking sites as pseudo-substrates; in either way, SOCS1 functions to block STAT1 from phosphorylation [52]. The wiring diagram also includes the Jak/STAT independent induction of STAT1 expression by IFN-γ. Figure 8B also gives a simplified wiring diagram to show the processes of slow STAT1 synthesis, STAT1 activation through covalent modification, and inhibition from SOCS1 whose synthesis is activated by STAT1. The system dynamics is then modeled by ODEs (see Table S1 and S2 for details).

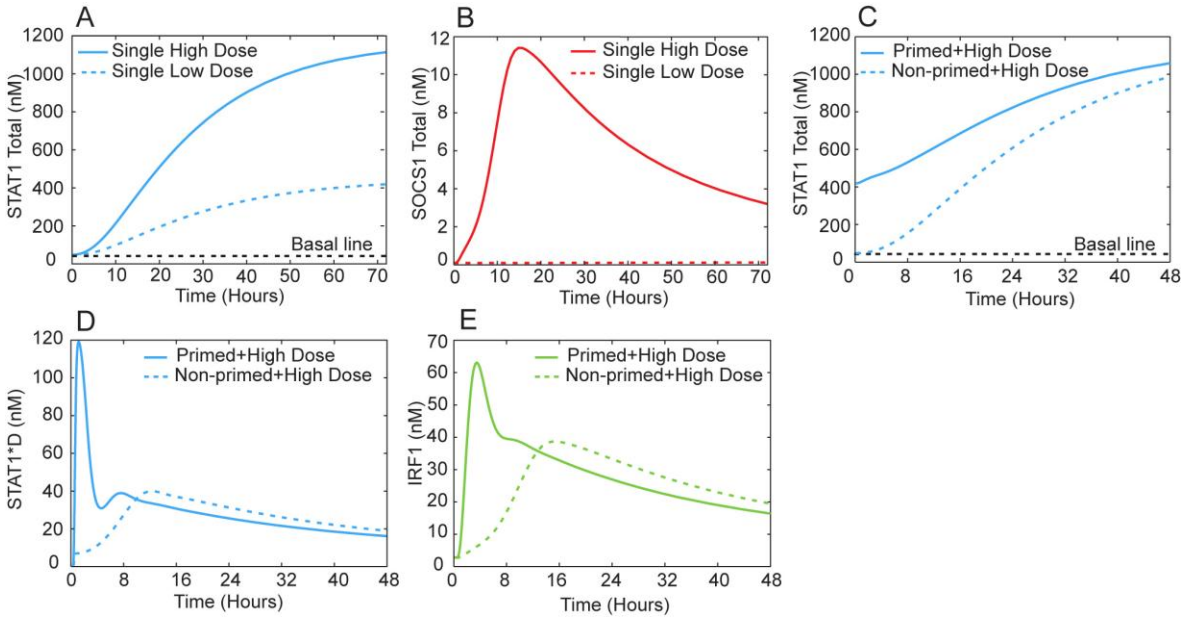

Figure 2.9 Simulated time course of the IFN-γ signaling network (A, B) Macrophages

were given 0.15 μg/L and 5 μg/L IFN-γ treatment for 72 hours, STAT1 responded quickly even at every low concentration while SOCS1 could only be turned on by high dose of IFN-γ; (C) Primed macrophages had an increased protein level of STAT1 ready for phosphorylation while non-primed macrophages still took time to accumulate equal amount of STAT1 (D); (D) Increased STAT1 in primed macrophages was rapidly activated by phosphorylation upon the second exposure to high concentration of IFN-γ; on the contrary, single high dose IFN-γ treatment of non-primed cells only initiated a slower and weaker STAT1 phosphorylation (D). The priming effect was also observed when Jak/STAT downstream gene, IRF-1, was examined (E).

Our computational analysis reveals a combination of the AI and PS mechanisms in this system. To illustrate, we see that under a 72 hour priming with LD IFN-γ (0.15 μg/L), the stimulated cells increase the expression of STAT1 but not SOCS1 (Figure 2.9A & 2.9B); this is because LD priming does not turn on phosphorylation or activation of STAT1 which is required for SOCS1 production. However, the increased expression of STAT1 under LD pretreatment expands the pool of STAT1 for phosphorylation in response to the following HD IFN-γ (5μg/L). Compared to protein binding/unbinding and covalent modifications such as phosphorylation, the gene expression process of STAT1 and SOCS1 is rather slow. Under a single HD, a fast Jak/STAT pathway signaling event quickly initializes SOCS1 gene expression, which resulting in the suppression of STAT1 phosphorylation. For primed cells, however, the STAT1 gene expression dynamics is accelerated while that of SOCS1 remains unchanged. Before SOCS1 starts to function, the increased total STAT1 proteins and the STAT1 phosphorylation can add cooperatively, leading to a higher level of phosphorylated STAT1 dimer (STAT1*D) than that under single HD (Figure 2.9D). Figure 8B also suggests the combined AI/PS mechanism through

the interplay among the three processes with different time scales. Our simulations suggest that the downstream genes such as IRF-1 also show priming effect (Figure 2.9E), which is in agreement with experimental observations [25].

Notice that in this model we only considered the coupling between IFN-γ induced STAT1 gene expression and the canonical Jak/STAT pathway. Figure 2.6 suggests a number of parallel pathways that may contribute to the observed IFN-γ priming effect. These pathways function together to make the temporal profile and amplitude of the priming phenomenon more complex.

d. Conclusions

Molecules within a cell interact with each other and form a large interconnected network. Consequently cellular information barely propagates linearly through a single pathway. The priming effect, which widely studied using immune cells, is such an example. Based on our previous *in silico* studies [48], in this work we proposed a generic procedure to identify possible candidates contributing to the priming effect through combined experimental time course measurement, subsequent data analysis and mathematical modeling. We demonstrated the procedure with high throughput microarray and other data on interferon-γ induced priming effects. This procedure is generally applicable to other similar problems. Especially it is of great significance to examine the generality and the specificity of the observed priming effects, in terms of stimulant and cell types. One may perform systematic screening using the proposed procedure combining with high throughput measurements, at both transcriptome and proteome levels.

e. Methods

Microarray data processing

The microarray data were downloaded from Gene Expression Omnibus (GEO, accession number: GDS1365). The data record the expression profile of approximately 12,000 gene probes with 3 independent pools. This is the only dataset we could find from GEO that include systematic time course measurement under either single dose or sequential stimulations (Control, HD 3hr, HD 24hr, LD Control, LD+HD 3hr, LD+HD 24hr. LD: 0.15 μg/L IFN-γ, HD: 5 μg/L IFN-γ).

In order to analyze the gene expression pattern, we first filtered out genes that contain no "Present Call" in all three independent pools. Genes that do not differentially express (by fold change < 2) under all of the following conditions were also filtered out: LD vs Control, HD (3hr) vs Control, HD (24hr) vs Control, LD+HD (3hr) vs Control and LD+HD (24hr) vs Control. All Differential expression was statistically analyzed by Welch's t-test with FDR correction. The threshold of p-value is set to be 0.05.

Network construction with the IPA database

We used the commercial database IPA® (@Ingenuity) to construct the molecular interactions networks of interested genes and products. IPA® assembles the signaling/regulatory networks on a literature basis. Database searching was restricted to immune cells and immune cell lines in *Mus musculus* or *Homo sapiens*. Interaction type was chosen to be either direct or indirect (i.e. interaction with intermediates). Prediction on potential priming candidates was made by comparing the priming motifs shown in Figure 2.2 and the signaling/ regulatory networks constructed by IPA®.

Detailed modeling with ordinary differential equations

We used a mathematic model adapted from Yamada et al. [51] to simulate the dynamics of Jak/STAT pathway in macrophages under different stimulation scenarios. Hu et al. have reported that increased expression of STAT1 induced by the first dose of IFN-γ treatment was responsible for sensitization of Jak/STAT1 pathway[25], we therefore added two more reactions to the original model: STAT1 transcription triggered by IFN-γ and STAT1translation. In addition, we introduced another two reactions describing IRF-1 transcription and translation. Adding these two reactions allows us to exam the expression behavior of downstream gene IRF-1for priming effects. As it is unclear how IFN-γ affects STAT1 expression, we proposed that an unknown intermediate X transduces the signal from IFN-γ to STAT1 gene.

As shown in Table S1 and Table S2, our model includes 36 variables and 50 parameters. Most of the rate equations are presented using Mass-action kinetics (Table S3). Several equations presenting gene transcription are denoted using Michaelis-Menten kinetics (Table S3). We employed the same initial conditions for Jak, IFN-γ receptor, PPX, PPN and SHP-2 as in the work of Yamada et al. Other initial conditions are set to be the steady-state values achieved given zero IFN-γ signal. These ODEs are solved using standard ODE solver in Matlab. In our simulation, macrophages were primed with 0.15μg/L IFN-γ for 3 days, after which cells were washed for 10 minutes with fresh medium and re-stimulated with 5μg/L IFN-γ for 2 days. The total STAT1 and SOCS1 proteins under repetitive two stimulations and single high dose of IFN-γ treatment were analyzed. In addition, phosphorylated STAT1 dimer and IRF-1 were examined as readouts to quantify the level of priming effect.

f. Acknowledgement

We thank Drs Xiaoyu Hu and Roderick Jensen for helpful discussions. This work was supported in part by the National Science Foundation (DMS), and by the National Institute of Allergy and Infectious Diseases (AI099120-01).

g. Supplementary Information

Table S1 Biochemical reactions and Parameters for the computational model

Biochemical reactions	Parameters	Notes
[R]+[JAK]↔[RJ]	k1=100	Adapted from Yamada's model [51].
	k_1=0.05	
[IFN-γ]+[RJ] ↔ [IFNRJ]	k2=20	
	k_2=0.02	
2[IFNRJ] ↔ [IFNRJ2]	k3=40	
	k_3=0.2	
[IFNRJ2]→[IFNRJ2*]	k4=0.005	
[IFNRJ2*]+[STAT1c] ↔ [IFNRJ2*-STAT1c]	k5=8	
	k_5=0.8	
[IFNRJ2*-STAT1c]→[IFNRJ2*]+[STAT1c*]	k6=0.4	
[IFNRJ2*]+[STAT1c*]↔[IFNRJ2*-STAT1c*]	k7=5	
	k_7=0.5	
2[STAT1c*]↔[STAT1c*-STAT1c*]	k8=20	
	k_8=0.1	
[IFNRJ2*]+[SHP-2] ↔[IFNRJ2*-SHP-2]	k9=1	
	k_9=0.2	
[IFNRJ2*-SHP-2]→[IFNRJ2]+[SHP-2]	k10=0.003	
[PPX]+[STAT1c*]↔[PPX-STAT1c*]	k11=1	
	k_11=0.2	
[PPX-STAT1c*]→[PPX]+[STAT1c]	k12=0.003	
[PPX]+[STAT1c*-STAT1c*]↔[PPX-STAT1c*-STAT1c*]	k11=1	
	k_11=0.2	
[PPX-STAT1c*-STAT1c*]→[PPX]+[STAT1c-STAT1c*]	k12=0.003	
[STAT1c]+[STAT1c*]↔[STAT1c-STAT1c*]	k13=0.0002	
	k_13=0.2	
[STAT1c*-STAT1c*]→[STAT1n*-STAT1n*]	k14 =0.005	
2[STAT1n*]↔[STAT1n*-STAT1n*]	k7=5	
	k_7=0.5	
[PPN]+[STAT1n*]↔[PPN-STAT1n*]	k15 =1	
	k_15 = 0.2	
[PPN-STAT1n*]→[PPN]+[STAT1n]	k16 =0.005	
[PPN]+[STAT1n*-STAT1n*]↔[PPN-STAT1n*-STAT1n*]	k15 =1	
	k_15 = 0.2	
[PPN-STAT1n*-STAT1n*]→[PPN]+[STAT1n-STAT1n*]	k16 =0.005	
[STAT1n]+[STAT1n*]↔[STAT1n-STAT1n*]	k13=0.0002	
	k_13=0.2	
[STAT1n]→[STAT1c]	k17 =0.05	
d[SOCS1_mRNAn]/dt =k18+k18a[STAT1n*-STAT1n*]/(k18b+[STAT1n*-STAT1n*])	k18=1×10^{-9}	Basal transcription rate of SOCS mRNA, fitted.
	k18a = 0.002 nM/s	Maximal SOCS1 mRNA transcription rate activated by STAT1, fitted.
	k18b = 400 nM	Adapted from Yamada's model [51].
[SOCS1_mRNAn]→[SOCS1_mRNAc]	k19 = 0.001	
d[SOCS1]/dt = k20[SOCS1_mRNAc]	k20 = 0.01	
[SOCS1]+[IFNRJ2*]↔[SOCS1-IFNRJ2*]	k21=20	
	k_21=0.1	

Table S1 (Cont'd)

Biochemical reactions	Parameters	Notes
d[SOCS1_mRNAc]/dt= -k22[SOCS1_mRNAc]	k22 =0.0008	SOCS1 mRNA degradation rate, fitted.
d[SOCS1]/dt= -k23[SOCS1]	k23 =0.00013	SOCS1 has a half-life of 1.5 hours [53].
[STAT1c]+[SOCS1-IFNRJ2*]↔[SOCS1-IFNRJ2*-STAT1c]	k5=8	Adapted from Yamada's model [51].
	k_5=0.8	
[SHP-2]+[SOCS1-IFNRJ2*-STAT1c]↔[SOCS1-IFNRJ2*-STAT1c-SHP-2]	k9=1	
	k_9=0.2	
[SOCS1-IFNRJ2*-STAT1c-SHP-2]→[SOCS1]+[IFNRJ2]+[STAT1c]+[SHP-2]	k10=0.003	
[SOCS1-IFNRJ2*-STAT1c-SHP-2]→[IFNRJ2*-STAT1c-SHP-2]	k23 =0.00013	SOCS1 has a half-life of 1.5 hours [53].
d[X]/dt=k24a[IFN-γ]/(k24b+[IFN-γ])-k_24[X]	k24a=5×10^{-6} nM/s	Maximal X expression rate stimulated by signal, fitted.
	k24b=0.016 nM	Michaelis-Menten constant, fitted.
	k_24=0.0002	X degradation rate, fitted.
d[STAT1_mRNA]/dt=k25+k25a[X]/(k25b+[X])-k_25[STAT1_mRNA]	k25=2×10^{-9}	STAT1 basal transcription rate, fitted.
	k25a=8×10-4 nM/s	Maximal STAT1 transcription rate stimulated by X, fitted.
	k25b=0.4 nM	Michaelis-Menten constant, fitted.
	k_25=0.000035	STAT1 mRNA has a half-life of about 7.4 hours [54].
d[STAT1]/dt=k26[STAT1_mRNA]-k_26[STAT1]	k26=0.01	STAT1 translation rate, fitted.
	k_26=0.000012	STAT1 has a half-life of 16 hours[53].
d[IRF1_mRNA/dt=k27a[STAT1n*-STAT1n*]/(k27b+[STAT1n*-STAT1n*])-k_27[IRF1_mRNA]	k27a=0.004 nM/s	Fitted
	k27b=400	Fitted
	k_27=0.00016	IRF1 mRNA has a half-life of 1.2 hours[54].
d[IRF1]/dt=k28[IRF1_mRNA]-k_28[IRF1]	k28=0.01	Fitted
	k_28=0.00038	IRF1 has a half-life of about 30 minutes[55].

*Initial condition: [R] =12nM, [Jak]=12nM, [SHP-2]=100nM, [PPX]=50nM and [PPN]=60nM

*The first and second order rate constants are expressed in units of $second^{-1}$ and 10^6 $molar^{-1}$ $second^{-1}$, respectively.

Table S2 Variables and Ordinary Differentiation Equations of the Computational Model

Variable Index	Gene-Symbol	Differentiation equation
S	IFN-γ	
x_1	R (IFN-γ Receptor)	$dx_1/dt = -k_1 \cdot x_1 \cdot x_2 + k_{-1} \cdot x_3$
x_2	JAK	$dx_2/dt = -k_1 \cdot x_1 \cdot x_2 + k_{-1} \cdot x_3$
x_3	RJ	$dx_3/dt = k_1 \cdot x_1 \cdot x_2 - k_{-1} \cdot x_3 - k_2 \cdot S \cdot x_3 + k_{-2} \cdot x_4$
x_4	IFNRJ	$dx_4/dt = k_2 \cdot S \cdot x_3 - k_{-2} \cdot x_4 - 2 \cdot k_3 \cdot x_4 \cdot x_4 + 2 \cdot k_{-3} \cdot x_5$
x_5	IFNRJ2	$dx_5/dt = k_3 \cdot x_4 \cdot x_4 - k_{-3} \cdot x_5 - k_4 \cdot x_5 + k_{10} \cdot x_{13} + k_{10} \cdot x_{31}$
x_6	IFNRJ2*	$dx_6/dt = k_4 \cdot x_5 - k_5 \cdot x_6 \cdot x_7 + k_{-5} \cdot x_8 + k_6 \cdot x_8 - k_7 \cdot x_6 \cdot x_9 + k_{-7} \cdot x_{10}$ $-k_9 \cdot x_6 \cdot x_{12} + k_{-9} \cdot x_{13} - k_{21} \cdot x_{28} \cdot x_6 + k_{-21} \cdot x_{29}$
x_7	STAT1c	$dx_7/dt = -k_5 \cdot x_6 \cdot x_7 + k_{-5} \cdot x_8 + k_{12} \cdot x_{15} - k_{13} \cdot x_7 \cdot x_9 + k_{-13} \cdot x_{17} + k_{17} \cdot x_{25}$ $-k_5 \cdot x_7 \cdot x_{29} + k_{-5} \cdot x_{30} + k_{10} \cdot x_{31} + k_{26} \cdot x_{33} - k_{-26} \cdot x_7$
x_8	IFNRJ2*-STAT1c	$dx_8/dt = k_5 \cdot x_6 \cdot x_7 - k_{-5} \cdot x_8 - k_6 \cdot x_8$
x_9	STAT1c*	$dx_9/dt = k_6 \cdot x_8 - k_7 \cdot x_6 \cdot x_9 + k_{-7} \cdot x_{10} - 2 \cdot k_8 \cdot x_9 \cdot x_9 + 2 \cdot k_{-8} \cdot x_{11}$ $-k_{11} \cdot x_{14} \cdot x_9 + k_{-11} \cdot x_{15} - k_{13} \cdot x_7 \cdot x_9 + k_{-13} \cdot x_{17}$
x_{10}	IFNRJ2*-STAT1c*	$dx_{10}/dt = k_7 \cdot x_6 \cdot x_9 - k_{-7} \cdot x_{10}$
x_{11}	STAT1c*-STAT1c*	$dx_{11}/dt = k_8 \cdot x_9 \cdot x_9 - k_{-8} \cdot x_{11} - k_{14} \cdot x_{11} - k_{11} \cdot x_{14} \cdot x_{11} + k_{-11} \cdot x_{16}$
x_{12}	SHP-2	$dx_{12}/dt = -k_9 \cdot x_6 \cdot x_{12} + k_{-9} \cdot x_{13} + k_{10} \cdot x_{13} - k_9 \cdot x_{12} \cdot x_{30} + k_{-9} \cdot x_{31} + k_{10} \cdot x_{31}$
x_{13}	IFNRJ2*-SHP-2	$dx_{13}/dt = k_9 \cdot x_6 \cdot x_{12} - k_{-9} \cdot x_{13} - k_{10} \cdot x_{13}$
x_{14}	PPX	$dx_{14}/dt = -k_{11} \cdot x_{14} \cdot x_9 + k_{-11} \cdot x_{15} + k_{12} \cdot x_{15} - k_{11} \cdot x_{14} \cdot x_{11} + k_{-11} \cdot x_{16} + k_{12} \cdot x_{16}$
x_{15}	PPX-STAT1c*	$dx_{15}/dt = k_{11} \cdot x_{14} \cdot x_9 - x_{-11} \cdot x_{15} - k_{12} \cdot x_{15}$
x_{16}	PPX-STAT1c*-STAT1c*	$dx_{16}/dt = k_{11} \cdot x_{14} \cdot x_{11} - k_{-11} \cdot x_{16} - k_{12} \cdot x_{16}$
x_{17}	STAT1c-STAT1c*	$dx_{17}/dt = k_{12} \cdot x_{16} + k_{13} \cdot x_7 \cdot x_9 - k_{-13} \cdot x_{17}$
x_{18}	STAT1n*	$dx_{18}/dt = -2 \cdot k_7 \cdot x_{18} \cdot x_{18} + 2 \cdot k_{-7} \cdot x_{19} - k_{15} \cdot x_{20} \cdot x_{18} + k_{-15} \cdot x_{21} - k_{13} \cdot x_{25} \cdot x_{18}$ $+k_{-13} \cdot x_{24}$
x_{19}	STAT1n*-STAT1n*	$dx_{19}/dt = k_{14} \cdot x_{11} + k_7 \cdot x_{18} \cdot x_{18} - k_{-7} \cdot x_{19} - k_{15} \cdot x_{20} \cdot x_{19} + k_{-15} \cdot x_{22}$
x_{20}	PPN	$dx_{20}/dt = -k_{15} \cdot x_{20} \cdot x_{18} + k_{-15} \cdot x_{21} + k_{16} \cdot x_{21} - k_{15} \cdot x_{20} \cdot x_{19} + k_{-15} \cdot x_{22} + k_{16} \cdot x_{22}$
x_{21}	PPN-STAT1n*	$dx_{21}/dt = k_{15} \cdot x_{20} \cdot x_{18} - k_{-15} \cdot x_{21} - k_{16} \cdot x_{21}$
x_{22}	PPN-STAT1n*-STAT1n*	$dx_{22}/dt = k_{15} \cdot x_{20} \cdot x_{19} - k_{-15} \cdot x_{22} - k_{16} \cdot x_{22}$
x_{23}	STAT1n-STAT1n	$dx_{23}/dt = 0$
x_{24}	STAT1n-STAT1n*	$dx_{24}/dt = k_{16} \cdot x_{22} + k_{13} \cdot x_{25} \cdot x_{18} - k_{-13} \cdot x_{24}$
x_{25}	STAT1n	$dx_{25}/dt = -k_{13} \cdot x_{25} \cdot x_{18} + k_{-13} \cdot x_{24} + k_{16} \cdot x_{21} - k_{17} \cdot x_{25}$
x_{26}	SOCS1_mRNAn	$dx_{26}/dt = k_{18} + k_{18a} \cdot x_{19} / (k_{18b} + x_{19}) - k_{19} \cdot x_{26}$

x_{27}	SOCS1_mRNAc	$dx_{27}/dt = k_{19}\cdot x_{26} - k_{22}\cdot x_{27}$
x_{28}	SOCS1	$dx_{28}/dt = k_{20}\cdot x_{27} - k_{21}\cdot x_{28}\cdot x_6 + k_{-21}\cdot x_{29} - k_{23}\cdot x_{28} + k_{10}\cdot x_{31}$
x_{29}	SOCS1-IFNRJ2*	$dx_{29}/dt = k_{21}\cdot x_{28}\cdot x_6 - k_{-21}\cdot x_{29} - k_5\cdot x_7\cdot x_{29} + k_{-5}\cdot x_{30}$
x_{30}	SOCS1-IFNRJ2*-STAT1c	$dx_{30}/dt = k_5\cdot x_7\cdot x_{29} - k_{-5}\cdot x_{30} - k_9\cdot x_{12}\cdot x_{30} + k_{-9}\cdot x_{31}$
x_{31}	SOCS1-IFNRJ2*-STAT1c-SHP-2	$dx_{31}/dt = k_9\cdot x_{12}\cdot x_{30} - k_{-9}\cdot x_{31} - k_{10}\cdot x_{31} - k_{23}\cdot x_{31}$
x_{32}	IFNRJ2*-STAT1c-SHP-2	$dx_{32}/dt = k_{23}\cdot x_{31}$
x_{33}	STAT1c_mRNA	$dx_{33}/dt = k_{25} + k_{25a}\cdot x_{36}/(k_{25b} + x_{36}) - k_{-25}\cdot x_{33}$
x_{34}	IRF1-mRNA	$dx_{34}/dt = k_{27a}\cdot x_{19}/(k_{27b} + x_{19}) - k_{-27}\cdot x_{34}$
x_{35}	IRF1	$dx_{35}/dt = k_{28}\cdot x_{34} - k_{-28}\cdot x_{35}$
x_{36}	X	$dx_{36}/dt = k_{24a}\cdot S/(k_{24b} + S) - k_{-24}\cdot x_{36}$

Table S3 Rate equations for each biochemical reaction

Biochemical reactions	Rate equations
[R]+[JAK]↔[RJ]	$x_1 + x_2 \xleftarrow[k_{-1}]{k_1} x_3$
[IFN-γ]+[RJ] ↔ [IFNRJ]	$S + x_3 \xleftarrow[k_{-2}]{k_2} x_4$
2[IFNRJ] ↔ [IFNRJ2]	$2 \cdot x_4 \xleftarrow[k_{-3}]{k_3} x_5$
[IFNRJ2]→[IFNRJ2*]	$x_5 \xrightarrow{k_4} x_6$
[IFNRJ2*]+[STAT1c] ↔ [IFNRJ2*-STAT1c]	$x_6 + x_7 \xleftarrow[k_{-5}]{k_5} x_8$
[IFNRJ2*-STAT1c]→[IFNRJ2*]+[STAT1c*]	$x_8 \xrightarrow{k_6} x_6 + x_9$
[IFNRJ2*]+[STAT1c*]↔[IFNRJ2*-STAT1c*]	$x_6 + x_9 \xleftarrow[k_{-7}]{k_7} x_{10}$
2[STAT1c*]↔[STAT1c*-STAT1c*]	$2 \cdot x_9 \xleftarrow[k_{-8}]{k_8} x_{11}$
[IFNRJ2*]+[SHP-2] ↔[IFNRJ2*-SHP-2]	$x_6 + x_{12} \xleftarrow[k_{-9}]{k_9} x_{13}$
[IFNRJ2*-SHP-2]→[IFNRJ2]+[SHP-2]	$x_{13} \xrightarrow{k_{10}} x_5 + x_{12}$
[PPX]+[STAT1c*]↔[PPX-STAT1c*]	$x_{14} + x_9 \xleftarrow[k_{-11}]{k_{11}} x_{15}$
[PPX-STAT1c*]→[PPX]+[STAT1c]	$x_{15} \xrightarrow{k_{12}} x_{14} + x_7$
[PPX]+[STAT1c*-STAT1c*]↔[PPX-STAT1c*-STAT1c*]	$x_{14} + x_{11} \xleftarrow[k_{-11}]{k_{11}} x_{16}$
[PPX-STAT1c*-STAT1c*]→[PPX]+[STAT1c-STAT1c*]	$x_{16} \xrightarrow{k_{12}} x_{14} + x_{17}$
[STAT1c]+[STAT1c*]↔[STAT1c-STAT1c*]	$x_7 + x_9 \xleftarrow[k_{-13}]{k_{13}} x_{17}$
[STAT1c*-STAT1c*]→[STAT1n*-STAT1n*]	$x_{11} \xrightarrow{k_{14}} x_{19}$
2[STAT1n*]↔[STAT1n*-STAT1n*]	$2 \cdot x_{18} \xleftarrow[k_{-7}]{k_7} x_{19}$
[PPN]+[STAT1n*]↔[PPN-STAT1n*]	$x_{20} + x_{18} \xleftarrow[k_{-15}]{k_{15}} x_{21}$
[PPN-STAT1n*]→[PPN]+[STAT1n]	$x_{21} \xrightarrow{k_{16}} x_{20} + x_{25}$
[PPN]+[STAT1n*-STAT1n*]↔[PPN-STAT1n*-STAT1n*]	$x_{20} + x_{19} \xleftarrow[k_{-15}]{k_{15}} x_{22}$
[PPN-STAT1n*-STAT1n*]→[PPN]+[STAT1n-STAT1n*]	$x_{22} \xrightarrow{k_{16}} x_{20} + x_{24}$
[STAT1n]+[STAT1n*]↔[STAT1n-STAT1n*]	$x_{25} + x_{18} \xleftarrow[k_{-13}]{k_{13}} x_{24}$
[STAT1n]→[STAT1c]	$x_{25} \xrightarrow{k_{17}} x_7$
d[SOCS1_mRNAn]/dt =k18+k18a[STAT1n*-STAT1n*]/(k18b+[STAT1n*-STAT1n*])	$dx_{26} / dt = k_{18} + k_{18a} \cdot x_{19} / (k_{18b} + k_{19})$
[SOCS1_mRNAn]→[SOCS1_mRNAc]	$x_{26} \xrightarrow{k_{19}} x_{27}$
d[SOCS1]/dt = k20[SOCS1_mRNAc]	$dx_{28} / dt = k_{20} \cdot x_{27}$
[SOCS1]+[IFNRJ2*]↔[SOCS1-IFNRJ2*]	$x_{28} + x_6 \xleftarrow[k_{-21}]{k_{21}} x_{29}$

d[SOCS1_mRNAc]/dt= -k22[SOCS1_mRNAc]	$dx_{27} / dt = -k_{22} \cdot x_{27}$
d[SOCS1]/dt= -k23[SOCS1]	$dx_{28} / dt = -k_{23} \cdot x_{28}$
[STAT1c]+[SOCS1-IFNRJ2*]↔[SOCS1-IFNRJ2*-STAT1c]	$x_7 + x_{29} \xleftrightarrow[k_{-5}]{k_5} x_{30}$
[SHP-2]+[SOCS1-IFNRJ2*-STAT1c]↔[SOCS1-IFNRJ2*-STAT1c-SHP-2]	$x_{12} + x_{30} \xleftrightarrow[k_{-9}]{k_9} x_{31}$
[SOCS1-IFNRJ2*-STAT1c-SHP-2]→[SOCS1]+[IFNRJ2]+[STAT1c]+[SHP-2]	$x_{31} \xrightarrow{k_{10}} x_{28} + x_4 + x_7 + x_{12}$
[SOCS1-IFNRJ2*-STAT1c-SHP-2]→[IFNRJ2*-STAT1c-SHP-2]	$x_{31} \xrightarrow{k_{23}} x_{30}$
d[X]/dt=k24a[IFN-γ]/(k24b+[IFN-γ])-k_24[X]	$dX / dt = k_{24a} \cdot S / (k_{24b} + S) - k_{-24} \cdot X$
d[STAT1_mRNA]/dt=k25+k25a[X]/(k25b+[X])-k_25[STAT1_mRNA]	$dx_{33} / dt = k_{25} + k_{25a} \cdot X / (k_{25b} + X) - k_{-25} \cdot x_{33}$
d[STAT1]/dt=k26[STAT1_mRNA]-k_26[STAT1]	$dx_7 / dt = k_{26} \cdot x_{33} - k_{-26} \cdot x_7$
d[IRF1_mRNA/dt=k27a[STAT1n*-STAT1n*]/(k27b+[STAT1n*-STAT1n*])-k_27[IRF1_mRNA]	$dx_{34} / dt = k_{27a} \cdot x_{19} / (k_{27b} + x_{19}) - k_{-27} \cdot x_{34}$
d[IRF1]/dt=k28[IRF1_mRNA]-k_28[IRF1]	$dx_{35} / dt = k_{28} \cdot x_{34} - k_{-28} \cdot x_{35}$

Figure S1.

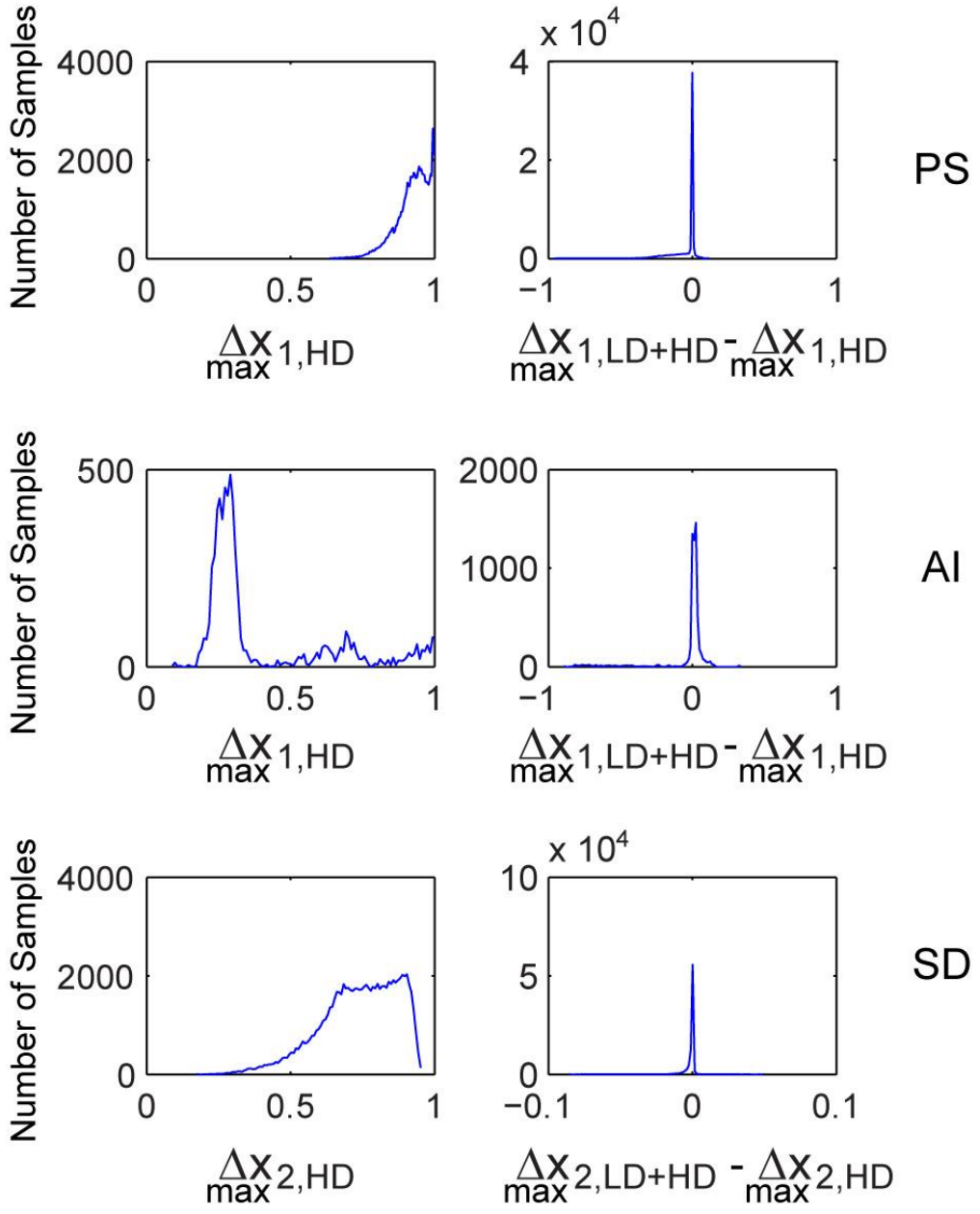

Figure S1 The maximum change distribution of regulators induced by HD or LD+HD under each priming mechanism. First column: Sample distribution in term of maximum change of x_1 or x_2 under HD alone (i.e., $\Delta_{\max} x_{i,HD}$). Second column: distribution of changes between the maximum induction under LD+HD and the maximum induction under HD alone

(i.e., $\underset{\max}{\Delta} x_{i,LD+HD} - \underset{\max}{\Delta} x_{i,HD}$). For PS and AI, there is a great increase in x_1 under HD, but the maximum expression of x_1 under LD+HD and HD alone shows no significant difference; Similarly for PS, x_2 expression is enhanced by HD, whereas maximum expression of x_2 under LD+HD is almost the same with that under HD alone.

Figure S2.

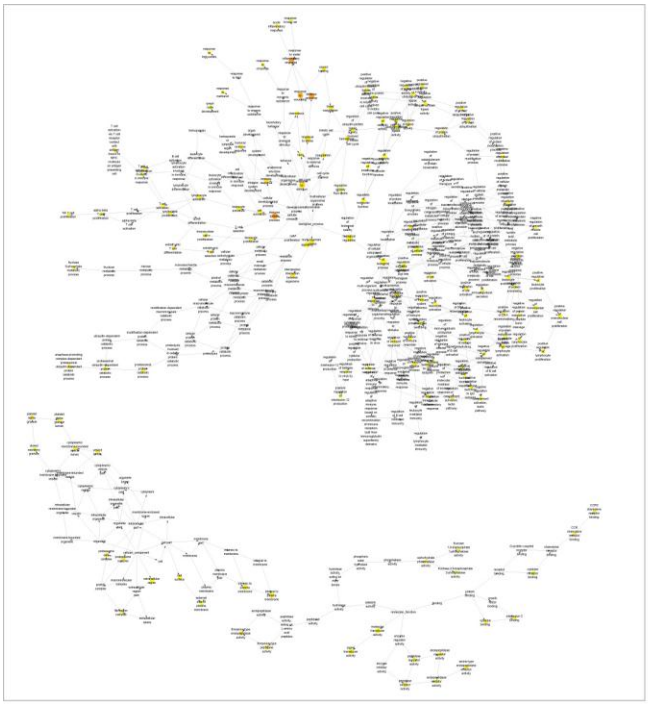

Low dose induced cellular function (top 10)

inflammatory response
defense response
immune system process
response to wounding
immune response
response to stimulus
response to stress
blood coagulation
coagulation
regulation of immune effector process

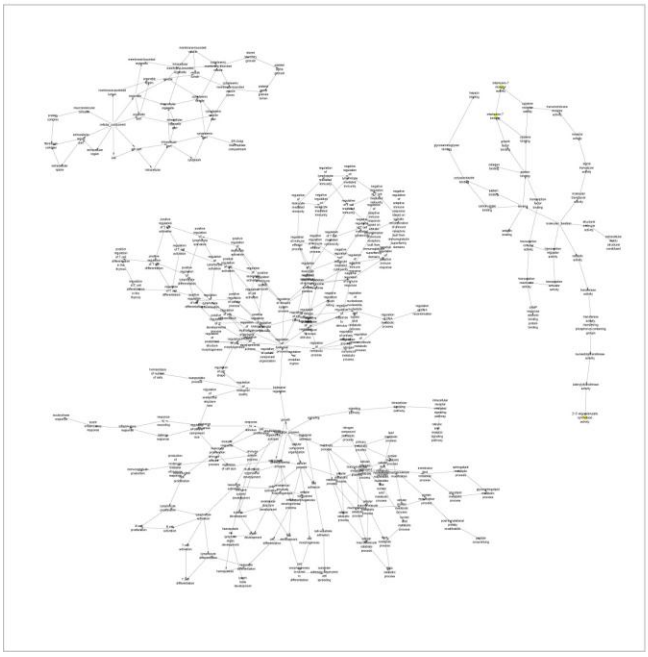

Low dose reduced cellular function (top 10)

IL7 receptor activity
IL7 binding
2'-5'-oligoadenylate synthetase activity
negative regulation of T cell mediated cytotoxicity
positive regulation of T cell differentitation in the thymus
cAMP repsonse element binding protein binding
negative regulation of leukocyte mediated cytotoxicity
negative regulation of T cell mediated immunity
negative regulation of cell killing
fibrinogen complex

Figure S2 Functional clustering over genes significant increased or decreased (⩾2 fold) under low dose of IFN-γ. The functional clustering is computed according to the enrichment of gene ontology retrieved from GOStat database. The top 10 significantly physiological functions

of either LD induced or LD reduced genes are listed on the right. The functional clustering is computed by Cytoscape plugin BiNGO 2.44.

h. Reference

1. St Pierre BA, Tidball JG: **Differential response of macrophage subpopulations to soleus muscle reloading after rat hindlimb suspension.** *J Appl Physiol* 1994, **77:**290-297.
2. Brulez H, Verbrugh H: **First-line defense mechanisms in the peritoneal cavity during peritoneal dialysis.** *Perit Dial Int* 1995, **15:**S24-S33.
3. Fiorentino D, Zlotnik A, Mosmann T, Howard M, O'Garra A: **IL-10 inhibits cytokine production by activated macrophages.** *J Immunol* 1991, **147:**3815-3822.
4. Shnyra A, Brewington R, Alipio A, Amura C, Morrison DC: **Reprogramming of Lipopolysaccharide-Primed Macrophages Is Controlled by a Counterbalanced Production of IL-10 and IL-12.** *J Immunol* 1998, **160:**3729-3736.
5. Unanue ER: **Antigen-Presenting Function of the Macrophage.** *Annu Rev Immunol* 1984, **2:**395-428.
6. Mosser DM, Edwards JP: **Exploring the full spectrum of macrophage activation.** *Nat Rev Immunol* 2008, **8:**958-969.
7. Medzhitov R: **Toll-like receptors and innate immunity.** *Nat Rev Immunol* 2001, **1:**135-145.
8. Dong C: **TH17 cells in development: an updated view of their molecular identity and genetic programming.** *Nat Rev Immunol* 2008, **8:**337-348.
9. Gordon S: **Alternative activation of macrophages.** *Nat Rev Immunol* 2003, **3:**23-35.
10. Odegaard JI, Chawla A: **Alternative Macrophage Activation and Metabolism.** *Annu Rev Pathol* 2011, **6:**275-297.

11. Schoenborn JR, Wilson CB: **Regulation of Interferon-γ During Innate and Adaptive Immune Responses.** In *Advances in Immunology. Volume* Volume 96. Edited by Frederick WA: Academic Press; 2007: 41-101

12. Schroder K, Hertzog PJ, Ravasi T, Hume DA: **Interferon-γ: an overview of signals, mechanisms and functions.** *J Leukoc Biol* 2004, **75:**163-189.

13. Ivashkiv L, Hu X: **Signaling by STATs.** *Arthritis Res Ther* 2004, **6:**159 - 168.

14. Darnell J, Kerr I, Stark G: **Jak-STAT pathways and transcriptional activation in response to IFNs and other extracellular signaling proteins.** *Science* 1994, **264:**1415-1421.

15. Platanias LC: **Mechanisms of type-I- and type-II-interferon-mediated signalling.** *Nat Rev Immunol* 2005, **5:**375-386.

16. Ulevitch RJ, Kline L, Schreiber RD, Pingel J, Amaldi I, Reith W, Mach B: **Hyperexpression of interferon-gamma-induced MHC class II genes associated with reorganization of the cytoskeleton.** *Am J Pathol* 1991, **139:**287-296.

17. Végh Z, Wang P, Váky F, Klein E: **Increased expression of MHC class I molecules on human cells after short time IFN-γ treatment.** *Mol Immunol* 1993, **30:**849-854.

18. Ikeda H, Old LJ, Schreiber RD: **The roles of IFNγ in protection against tumor development and cancer immunoediting.** *Cytokine & growth factor reviews* 2002, **13:**95-109.

19. Ivashkiv LB, Hu X: **The JAK/STAT pathway in rheumatoid arthritis: Pathogenic or protective?** *Arthritis Rheum* 2003, **48:**2092-2096.

20. Rawlings JS, Rosler KM, Harrison DA: **The JAK/STAT signaling pathway.** *J Cell Sci* 2004, **117:**1281-1283.

21. Wang S, Koromilas A: **Stat1 is an inhibitor of Ras-MAPK signaling and Rho small GTPase expression with implications in the transcriptional signature of Ras transformed cells.** *Cell Cycle* 2009, **8:**2070-2079.

22. Hu X, Park-Min KH, Ho HH, Ivashkiv LB: **IFN-gamma-primed macrophages exhibit increased CCR2-dependent migration and altered IFN-gamma responses mediated by Stat1.** *J Immunol* 2005, **175:**3637-3647.

23. Krebs DL, Hilton DJ: **SOCS Proteins: Negative Regulators of Cytokine Signaling.** *STEM CELLS* 2001, **19:**378-387.

24. Yoshimura A, Naka T, Kubo M: **SOCS proteins, cytokine signalling and immune regulation.** *Nat Rev Immunol* 2007, **7:**454-465.

25. Hu X, Herrero C, Li W-P, Antoniv TT, Falck-Pedersen E, Koch AE, Woods JM, Haines GK, Ivashkiv LB: **Sensitization of IFN-[gamma] Jak-STAT signaling during macrophage activation.** *Nat Immunol* 2002, **3:**859-866.

26. Hu X, Chakravarty SD, Ivashkiv LB: **Regulation of interferon and Toll-like receptor signaling during macrophage activation by opposing feedforward and feedback inhibition mechanisms.** *Immunol Rev* 2008, **226:**41-56.

27. Gardy JL, Lynn DJ, Brinkman FSL, Hancock REW: **Enabling a systems biology approach to immunology: focus on innate immunity.** *Trends Immunol* 2009, **30:**249-262.

28. Gordon S, Martinez FO: **Alternative Activation of Macrophages: Mechanism and Functions.** *Immunity* 2010, **32:**593-604.

29. Akira S, Takeda K: **Toll-like receptor signalling.** *Nat Rev Immunol* 2004, **4:**499-511.

30. Hu X, Ivashkiv LB: **Cross-regulation of Signaling Pathways by Interferon-[gamma]: Implications for Immune Responses and Autoimmune Diseases.** *Immunity* 2009, **31:**539-550.

31. Tyson JJ, Chen K, Novak B: **Network dynamics and cell physiology.** *Nat Rev Mol Cell Biol* 2001, **2:**908-916.

32. Tyson JJ, Chen KC, Novak B: **Sniffers, buzzers, toggles and blinkers: dynamics of regulatory and signaling pathways in the cell.** *Curr Opin Cell Biol* 2003, **15:**221-231.

33. Alon U: *An introduction to systems biology: Design principles of biological circuits.* 1 edn: Chapman and Hall/CRC; 2007.

34. Natarajan M, Lin KM, Hsueh RC, Sternweis PC, Ranganathan R: **A global analysis of cross-talk in a mammalian cellular signalling network.** *Nat Cell Biol* 2006, **8:**571-580.

35. Cohen AA, Kalisky T, Mayo A, Geva-Zatorsky N, Danon T, Issaeva I, Kopito RB, Perzov N, Milo R, Sigal A, Alon U: **Protein dynamics in individual human cells: experiment and theory.** *PLoS ONE* 2009, **4:**e4901.

36. Zhang XK, Morrison DC: **Lipopolysaccharide-Induced Selective Priming Effects on Tumor-Necrosis-Factor-Alpha and Nitric-Oxide Production in Mouse Peritoneal-Macrophages.** *J Exp Med* 1993, **177:**511-516.

37. West MA, Koons A: **Endotoxin tolerance in sepsis: concentration-dependent augmentation or inhibition of LPS-stimulated macrophage TNF secretion by LPS pretreatment.** *J Trauma* 2008, **65:**893-898; discussion 898-900.

38. Shnyra A, Brewington R, Alipio A, Amura C, Morrison DC: **Reprogramming of lipopolysaccharide-primed macrophages is controlled by a counterbalanced production of IL-10 and IL-12.** *J Immunol* 1998, **160:**3729-3736.

39. Hirohashi N, Morrison DC: **Low-dose lipopolysaccharide (LPS) pretreatment of mouse macrophages modulates LPS-dependent interleukin-6 production in vitro.** *Infect Immun* 1996, **64:**1011-1015.

40. Henricson BE, Manthey CL, Perera PY, Hamilton TA, Vogel SN: **Dissociation of lipopolysaccharide (LPS)-inducible gene expression in murine macrophages pretreated with smooth LPS versus monophosphoryl lipid A.** *Infect Immun* 1993, **61:**2325-2333.

41. Moreno-Navarrete JM, Manco M, Ibanez J, Garcia-Fuentes E, Ortega F, Gorostiaga E, Vendrell J, Izquierdo M, Martinez C, Nolfe G, et al: **Metabolic endotoxemia and saturated fat contribute to circulating NGAL concentrations in subjects with insulin resistance.** *Int J Obes (Lond)* 2010, **34:**240-249.

42. Kiechl S, Egger G, Mayr M, Wiedermann CJ, Bonora E, Oberhollenzer F, Muggeo M, Xu Q, Wick G, Poewe W, Willeit J: **Chronic Infections and the Risk of Carotid Atherosclerosis : Prospective Results From a Large Population Study.** *Circulation* 2001, **103:**1064-1070.

43. Wiesner P, Choi SH, Almazan F, Benner C, Huang W, Diehl CJ, Gonen A, Butler S, Witztum JL, Glass CK, Miller YI: **Low doses of lipopolysaccharide and minimally oxidized low-density lipoprotein cooperatively activate macrophages via nuclear factor kappa B and activator protein-1: possible mechanism for acceleration of atherosclerosis by subclinical endotoxemia.** *Circ Res* 2010, **107:**56-65.

44. Slofstra S, Cate H, Spek CA: **Low dose endotoxin priming is accountable for coagulation abnormalities and organ damage observed in the Shwartzman reaction.**

A comparison between a single-dose endotoxemia model and a double-hit endotoxin-induced Shwartzman reaction. *Thromb J* 2006, **4:**13.

45. Cani PD, Amar J, Iglesias MA, Poggi M, Knauf C, Bastelica D, Neyrinck AM, Fava F, Tuohy KM, Chabo C, et al: **Metabolic endotoxemia initiates obesity and insulin resistance.** *Diabetes* 2007, **56:**1761-1772.

46. Cani PD, Bibiloni R, Knauf C, Waget A, Neyrinck AM, Delzenne NM, Burcelin R: **Changes in gut microbiota control metabolic endotoxemia-induced inflammation in high-fat diet-induced obesity and diabetes in mice.** *Diabetes* 2008.

47. Schroder K, Hertzog PJ, Ravasi T, Hume DA: **Interferon-gamma: an overview of signals, mechanisms and functions.** *J Leukoc Biol* 2004, **75:**163-189.

48. Fu Y, Glaros T, Zhu M, Wang P, Wu Z, Tyson JJ, Li L, Xing J: **Network Topologies and Dynamics Leading to Endotoxin Tolerance and Priming in Innate Immune Cells.** *PLoS Comp Biol (In print)* 2012.

49. Sunahori K, Yamamura M, Yamana J, Takasugi K, Kawashima M, Yamamoto H, Chazin WJ, Nakatani Y, Yui S, Makino H: **The S100A8/A9 heterodimer amplifies proinflammatory cytokine production by macrophages via activation of nuclear factor kappa B and p38 mitogen-activated protein kinase in rheumatoid arthritis.** *Arthritis Res Ther* 2006, **8:**R69.

50. Asao H, Okuyama C, Kumaki S, Ishii N, Tsuchiya S, Foster D, Sugamura K: **Cutting edge: the common gamma-chain is an indispensable subunit of the IL-21 receptor complex.** *J Immunol* 2001, **167:**1-5.

51. Yamada S, Shiono S, Joo A, Yoshimura A: **Control mechanism of JAK/STAT signal transduction pathway.** *FEBS Lett* 2003, **534:**190-196.

52. Yoshimura A, Naka T, Kubo M: **SOCS proteins, cytokine signalling and immune regulation.** *Nat Rev Immunol* 2007, **7:**454-465.

53. Siewert E, Muller-Esterl W, Starr R, Heinrich PC, Schaper F: **Different protein turnover of interleukin-6-type cytokine signalling components.** *European journal of biochemistry / FEBS* 1999, **265:**251-257.

54. Sharova LV, Sharov AA, Nedorezov T, Piao Y, Shaik N, Ko MSH: **Database for mRNA Half-Life of 19 977 Genes Obtained by DNA Microarray Analysis of Pluripotent and Differentiating Mouse Embryonic Stem Cells.** *DNA Research* 2009, **16:**45-58.

55. Watanabe N, Sakakibara J, Hovanessian AG, Taniguchi T, Fujita T: **Activation of IFN-β element by IRF-1 requires a post-translational event in addition to IRF-1 synthesis.** *Nucleic Acids Res* 1991, **19:**4421-4428.

56. Wong LH, Sim H, Chatterjee-Kishore M, Hatzinisiriou I, Devenish RJ, Stark G, Ralph SJ: **Isolation and Characterization of a Human STAT1Gene Regulatory Element.** *J Biol Chem* 2002, **277:**19408-19417.

57. Nguyen H, Lin R, Hiscott J: **Activation of multiple growth regulatory genes following inducible expression of IRF-1 or IRF/RelA fusion proteins.** *Oncogene* 1997, **15:**1425-1435.

58. Tyson JJ, Chen KC, Novak B: **Sniffers, buzzers, toggles and blinkers: dynamics of regulatory and signaling pathways in the cell.** *Curr Opin Cell Biol* 2003, **15:**221-231.

59. Ferrell Jr JE: **Self-perpetuating states in signal transduction: positive feedback, double-negative feedback and bistability.** *Curr Opin Cell Biol* 2002, **14:**140-148.

60. Geva-Zatorsky N, Dekel E, Cohen AA, Danon T, Cohen L, Alon U: **Protein Dynamics in Drug Combinations: a Linear Superposition of Individual-Drug Responses.** *Cell* 2010, **140:**643-651.

Chapter 3

Conclusion and Future work

In this work, we mainly focused on a nonlinear cell response under repetitive stimuli, the IFN-γ induced priming effect during macrophages activation. Such nonlinear response is quite a common phenomenon in biology system as even every single cell bears complicate regulation networks that constantly react to different extracellular and intracellular signals. This actually offers an innovative perspective for drug development and diseases treatment because single dose of medication treatment barely works whereas continuous intakes of two or more different drugs with certain frequency do help. Here we showed how to utilize some bioinformatics and statistics tools to design a strategy that one could use for microarray data analysis to search for potential candidates genes that may be engaged in priming effects. The analysis procedure developed in this paper is of significance as it may be extended to apply to many similar biology problems as well. Especially for the researchers who are doing large scale genes or proteins screen, our method can assist to narrow down and determine on which gene or protein they should be more concentrated for further investigation. For the specific topic on IFN-γ priming effect, we found that many genes could be potentially involved in the molecular network. Next, we set up a detailed mathematical model to reveal the underlying mechanism regulating IFN-γ mediated priming effect and eventually we found that this priming process follows both "activator induction" and "pathway synergy" mechanisms. These results provide us a guideline to design experiments to further confirm the priming mechanisms we proposed.

Although the priming effect in macrophages or monocytes has been widely studied, it is still unclear whether this is an intercellular or intracellular phenomenon. In other words, the

priming effect may be due to intracellular pathways cross-talks as we have hypothesized or intercellular interaction (Figure 3.1). When performing experiments with a bulk of cells, one cannot avoid cell-to-cell communication, like autocrine and paracrine.

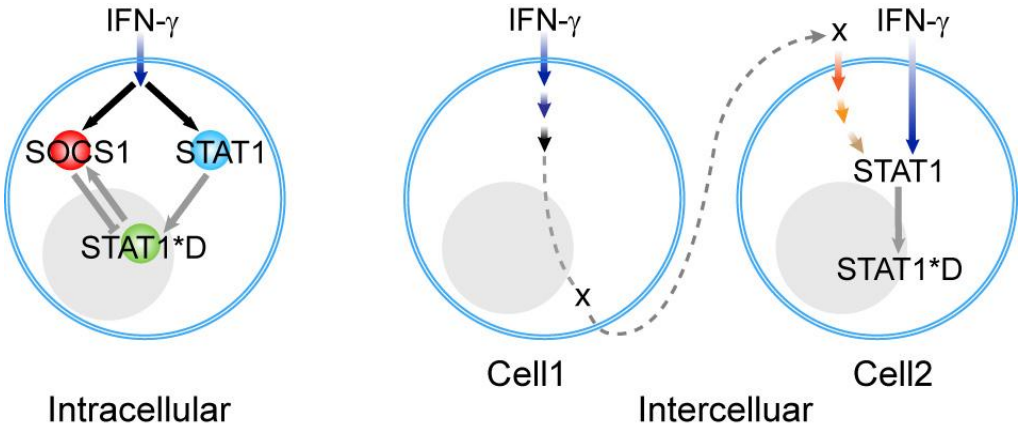

Figure 3.1 Priming can be either intracellular or intercellular cell response

Probably, the first dose stimulation actually induces cells to produce certain exogenous substance that serves as an extracellular signal acting on neighbor cells; so when receiving the second dose of stimulation, each cell basically has to react to two different signals, therefore reaching an enhanced cellular response (Figure 3.1). To clarify the real situation, single cell analysis may be required. For instance, we can focus on only one cell and check whether two subsequent stimulations would induce this cell to respond cooperatively. On the other hand, as discussed before, SOCS1 as a downstream target of STAT1 can feedback on STAT1 to suppress its phosphorylation, typically forming a negative feedback loop. In addition, it was also reported that IRF-1, which is a target gene of STAT1 and is up-regulated by IFN-γ stimulation, acts backwards to bind to the enhancer region of STAT1 gene and increase the expression of STAT1 at mRNA level [56, 57] (Figure 3.2A).

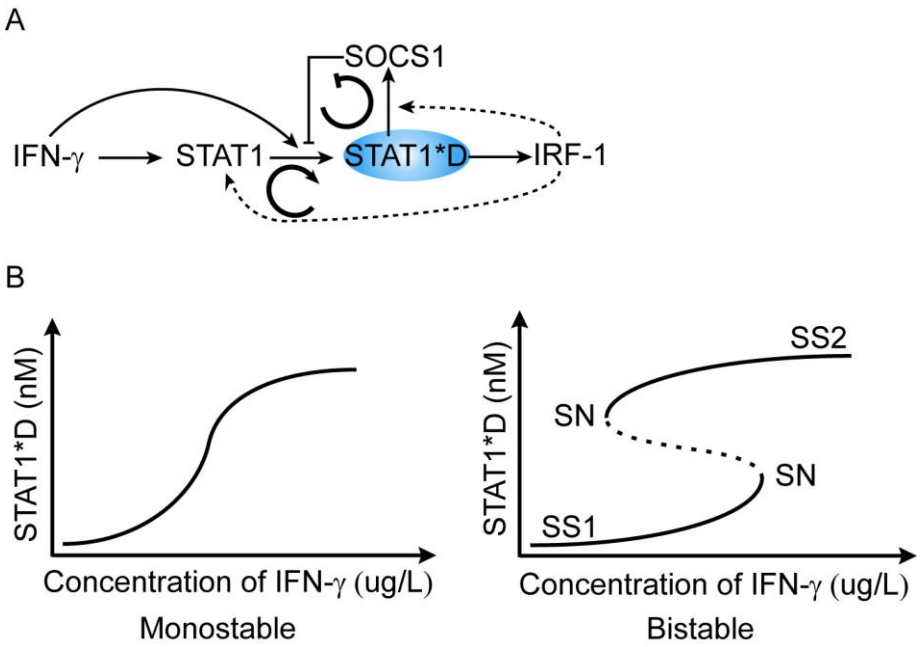

Figure 3.2 Feedback regulations predict bistable dynamics of Jak/STAT system (A) Both positive and negative feedback loops are involved in regulating Jak/STAT1 pathway. (B) Jak/STAT pathway can be either a monostable (left) or a bistable (right) system in terms of phosphorylated STAT1 dimer.

It is evident that these two genes and their encoded proteins, two pivotal transcription factors, construct an intracellular amplifier circuit or positive feedback loop that functions to regulate cellular responsiveness to the IFN-γ [56]. Actually, in vivo, this positive feedback loop may be responsible for the second wave transcription of STAT1 target genes after IFN-γ induction [22]. Regulation by negative and positive feedback is a hallmark of bifurcation system [58, 59]. Bifurcation refers to that, giving IFN-γ priming as an example, macrophages have two steady states in terms of STAT1 transcriptional activity with each cell having either a low or high STAT1 activity exclusively (Figure 3.2B). Physiologically, bistable dynamics could play significant roles because of that within a certain range of pathogen stimulation, a relatively low

macrophage activity is enough to clear infecting pathogens; but if comes a very high stimulation or pathogen assault, macrophages are quickly activated to a higher level steady state with largely increased phosphorylated STAT1 to get rid of pathogens. And even if pathogens are decreased a little bit, but macrophage activity still stays at the higher steady state until pathogens were cleared or decreased to a certain threshold. Basically, it helps to make sure that macrophages clear invading microbes quickly without causing any damage to host tissues. However, it is unrealistic to identify whether it is a monostable or bistable system because the readout measured is the average of a bulk of cells. Therefore by the same token, single cell analysis is required to determine whether it is a bistable system or not. We can do flow cytometry analysis using phosphorylated STAT1 dimer as a marker to exam the distribution of cells based on their transcriptional activity. If a bimodal distribution is observed, we can claim this priming process has bistable dynamics, and vice versa. Moreover, priming effect discussed in this paper mainly focus on two sequential treatments of the same signals, however, it would be also exciting to reveal the nonlinear effects of several different signals stimulation on cells, which would be another new area of cross-priming. In 2010, Uri Alon's group reported that protein dynamics by a combination of several drugs are actually a linear superposition of individual drug responses[60]. It seems that repetitively different stimuli treatments on cells may lead to more interesting cellular cell response.

Technically, computational analysis of biology problems is much more efficient and it works rather as a promising guideline for experimental design and investigation of systematic biology. I would say computational skills such as mathematical modeling, system biology simulation and bioinformatics is to become more and more important tools that infiltrate in life sciences research areas.